CHEMICAL REVIEWS

Volume 104, Number 12

# Role of the Surface in Luminescent Processes

Billie L. Abrams*,† and Paul H. Holloway‡

*Sandia National Laboratories, P.O. Box 5800-1421, Albuquerque, New Mexico 87185, and Department of Materials Science and Engineering, University of Florida, P.O. Box 116400, Gainesville, Florida 32611-6400*

*Received December 19, 2002*

## Contents



## 1. Introduction

### 1.1. Brief Historical Perspective

Luminescent phenomena have been observed from the earliest times. References to light emission from glowworms and fireflies lay embedded in ancient Chinese poetry as well as holy manuscripts (the Vedas) from Ancient India.[1] Aristotle (384−322 B.C.) and other philosophers of Ancient Greece documented luminescence from bacteria and fungus.[1] Continuing through the centuries, various stories of light coming from inanimate objects were told. Some of these descriptions have made researchers suspect electroluminescence as the source.[1] In the 17th and 18th centuries, more observations and discoveries were made including luminescence from inorganic materials. These materials were given the name "phosphors". The various types of luminescence were categorized in the 19th century as chemiluminescence, thermoluminescence, electroluminescence, photoluminescence, and radioluminescence, which included cathodoluminescence, anodoluminescence, and luminescence from X-rays and $\gamma$-rays.[1]

### 1.2. Importance of Surfaces in Luminescence

Through the 20th century, the luminescent mechanisms and phosphors have been investigated in more detail. Phosphors are currently defined as materials that convert various types of energy into electromagnetic radiation.[2]

Many of the mechanisms and theories of luminescence have depicted the phosphor as an infinite crystal. As a result, the crystal surface has often been neglected. Research has, for a long time, been focused mainly on the bulk luminescent and electronic processes within the phosphor material. These properties are, of course, a very important aspect of luminescence since they have led to a deep mechanistic understanding. However, the picture is incomplete without incorporating the effects of surfaces on luminescence. More recently, the research focus has shifted to include the role of the surface on luminescent processes. Perhaps the driving force for increased surface investigations of luminescent materials stems from demands from certain applications

† Sandia National Laboratories.
‡ University of Florida.

10.1021/cr020351r CCC: $48.50 
Published on Web 10/06/2004

Billie L. Abrams graduated with her Ph.D. in materials science and engineering from the University of Florida, Gainesville, FL, in December 2001. Billie worked on the degradation of FED phosphors under the guidance of Dr. Paul H. Holloway. She analyzed the surface chemistry reactions leading to luminescent degradation of cathodoluminescent phosphors using an electron beam probe. She has published several papers in the area as well as presented the work at several international conferences. Billie continued working in this area as well as guiding students during a postdoctoral term under Paul Holloway in 2001. She has won several awards including the EMPD Postdoctoal Award at the 2002 AVS, the Graduate Student Award at the 1999 AVS, and numerous travel scholarships to attend conferences. Billie Abrams is currently a Postdoctoral Associate at Sandia National Laboratories. She is now working in the area of nanoparticle synthesis of luminescent materials for applications in solid-state lighting. She is also applying techniques in analytical chemistry and nanocluster synthesis of semiconductors and metals for other applications such as photocatalysis and hydrogen production for use in fuel cells.

Paul H. Holloway is Distinguished Professor of Materials Science and Engineering and Director of MICROFABRITECH at the University of Florida, Gainesville, FL. He received a Ph.D. in materials engineering from Rensselaer Polytechnic Institute, Troy, NY, in 1972. He worked for General Electric Co. in Schenectady, NY, and at Sandia National Laboratories in Albuquerque, NM, prior to joining the University of Florida in 1978. He has served in numerous chapter and national offices of the American Vacuum Society including national President-Elect, President, and Past-President from 1986 to 1988. He is editor of *Critical Reviews in Solid State and Materials Sciences*, and serves on the Editorial Boards of both *Surface Science* and *Surface Science Spectra*. He has served on the Editorial Boards of the *Journal of Vacuum Science and Technology* and *Surface and Interface Analysis*. He was elected a Fellow of the AVS in 1993 and a lifetime Honorary Member of the AVS in 1997 and received the Albert Nerken Award in 1999. He is a Fellow of ASM International. His areas of interest are surfaces and interfaces in electronic and luminescent materials, particularly in thin film form. He has also studied gas/solid interactions relative to oxidation, corrosion, deposition, and etching. He has published over 300 papers, 5 book chapters, 5 books, and 5 patents, with several pending.

such as displays (fields emission displays (FEDs), vacuum fluorescent displays (VFDs), alternationg current thin film electroluminescent displays (ACT-FELs)), as well as more in-depth understanding of surface properties from studies of solids such as semiconductors.

Although there is considerable knowledge about the surface properties of semiconductors, it is not always directly applicable to phosphors. This is due mainly to the fact that semiconductors are usually band edge recombination materials whereas phosphors are state-to-state recombination materials.[3] In essence, recombination in semiconductors occurs via electrons and holes in the valence or conduction bands, or in excitonic states near these band edges. Doping and excitonic states are normally within a few $kT$ of the band edges (~30 meV).[3] In contrast, phosphors often depend on radiative relaxation from an excited to a ground state, localized on an activator site and lying deep within the band gap. It is true that there are some phosphors that depend on electron trapping on deep donor and deep acceptor sites which de-excite by radiative recombination. The energies of these sites are far (~1 eV) from the conduction and valence band edge energies, and therefore, the recombination is still distinct from band edge recombinations.[3] Various recombination transitions between excited and ground states are shown in Figure 1.[4] Due to the differences in recombination mechanisms between conventional semiconductors and phosphors, care will be used in drawing conclusions, but general comparisons may still be valid. It is the purpose of this review to explore in greater depth the effects of surfaces on luminescence.

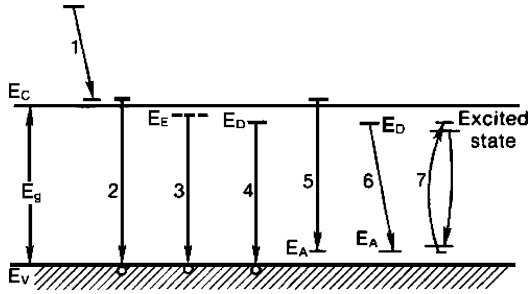


**Figure 1.** Luminescence transitions between the conduction and valence bands (2), from or to near-band edge states (3−5), from deep acceptor to deep donor states (6), or from excited to lower energy (ground) states (7). Reprinted with permission from ref 4. Copyright 1992 Manning Publications Inc.

In doing so, many aspects of the surface will be considered such as the structure, chemistry, and band gap. Research relating to fundamental surface science as well as current work in the areas of luminescent materials will be presented in an attempt to provide an overall picture of the role of surfaces in luminescence.

## 2. General Aspects and Properties of Surfaces

### 2.1. Surface Structure

A surface can be categorized as a two-dimensional (2-D) planar defect containing dangling bonds.[5] A surface signifies an abrupt change in the material properties as a function of distance perpendicular to

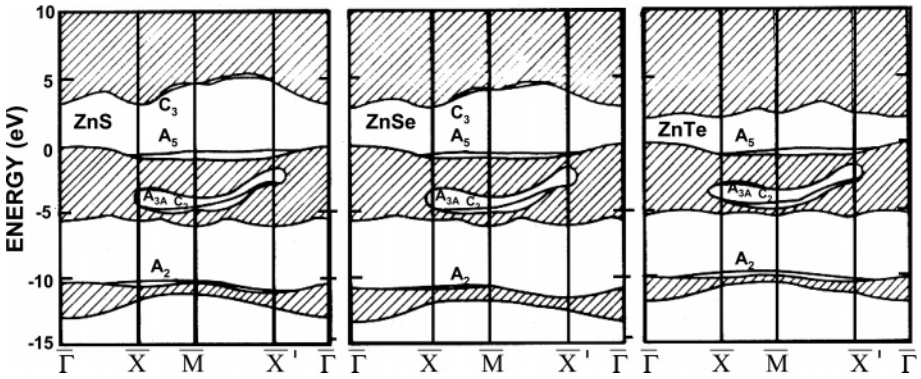


**Figure 2.** Surface state energy dispersion on ZnS(110), ZnSe(110), and ZnTe(110) surfaces. Reprinted with permission from ref 11. Copyright 1994 Elsevier.

the surface.[6] The presence of a surface is a deviation from the typically ordered crystal structure, which will lead to a change in luminescent characteristics. In general, radiative mechanisms compete with nonradiative mechanisms, and the surface is most often associated with nonradiative recombination and quenching of the luminescent mechanisms.[7]

The dimensions of the surface are dependent on several properties including atomic arrangement, composition, surface topography, adsorbed gas, surface treatment, and contamination.[6] Surface crystallography, phase formation, and defects must all be considered. The atoms may be arranged differently on the solid surface due to a termination of the bulk.[3,6] In regard to luminescence, composition in the plane of the surface and depth distribution are important factors. Embodied in composition are other properties such as surface segregation, adsorption, desorption, and compound and phase formation.[6]

It is quite common for the composition of the surface of a solid to be different from that of the bulk. This is known as surface segregation, and results from two thermodynamic energy effects. First, the surface energy of a solid is a function of composition,[6] and if a component of a binary or higher solid results in a lower surface energy, it is expected to concentrate on the surface. Furthermore, if the dilute component of a binary or ternary solid strains the host lattice (e.g., an activator with a radius larger or smaller than the atom it replaces in the phosphor host lattice), it will result in a higher energy state. The energy of the solid would be reduced by segregation of the activator to the surface, which is a region where strain can relax. Segregation of constituents of a phosphor have been reported[8] on the basis of the color shift observed during cathodoluminescence from $Y_2O_3$:3% Eu for lower primary electron beam energy. As reported by Jones et al.,[8] when the electron energy was reduced from 4 to 0.5 keV, the $x$ color coordinate decreased from 0.62 to 0.64 to ~0.59 for both pulsed laser deposited thin films and commercially produced powders. On the basis of the shift of CIE color coordinates for $Y_2O_3$:Eu by Ozawa,[9] this shift in the $x$ color coordinates suggests a Eu surface concentration between 2.25% and 2.5% versus 3% in the bulk. The CIE chromaticity diagram is used to verify optimal color saturation via color coordinates. On the basis of the good match of the size of Eu and Y ions, this surface depletion must be driven by an increase in the surface energy upon addition of Eu rather than due to strain energy.

In addition to surface composition, the topography may affect luminescence by geometric effects. Scattering occurs as a result of surface roughness. In most cases the surface has a detrimental effect; however, some researchers have experienced luminescent enhancement (as will be discussed in section 6.3). Other aspects of topography include facets, area, and phase distribution.

Some luminescence mechanisms are more sensitive to certain surface properties. For example, cathodoluminescence (CL) may be more sensitive to surface contamination at low versus high accelerating voltages since the luminescent excitation depth decreases as the electron beam energy is reduced. As a result, surface atomic and molecular dynamics, such as chemical reactions, vibration, diffusion, and evaporation, become important. Surface electronic structure is also important for most types of luminescent processes. It would seem desirable to have a clean surface free of defects since the electronic structure can easily be modified by adsorbates.

In general, the role of surface defects is important in luminescence. They can lead to a variety of phenomena including creation of impurity quantum states in the band gap, increased scattering leading to a reduction in carrier mobility, and change in excess carrier recombination rates in luminescence processes.[5]

## 2.2. Band Structure

The solid-state band gap of the surface differs from that of the bulk. Instead of the three-dimensional energy band, there are two-dimensional energy bands describing the surface.[10] The widths of these surface bands are generally thought to be narrower than those describing bulk phosphors.[10] This may have an effect on the emission of photons or, more specifically, affect their energy.

Some researchers have used angle-resolved photoelectron spectroscopy in an attempt to measure the surface band structure. However, it is difficult to distinguish band edge from surface state photoemission.[10,11] Ferraz et al. calculated the (110) surface band structures of three different II−VI semiconductors: ZnS, ZnSe, and ZnTe.[11] These band structures are shown in Figure 2. Note the surface states in the

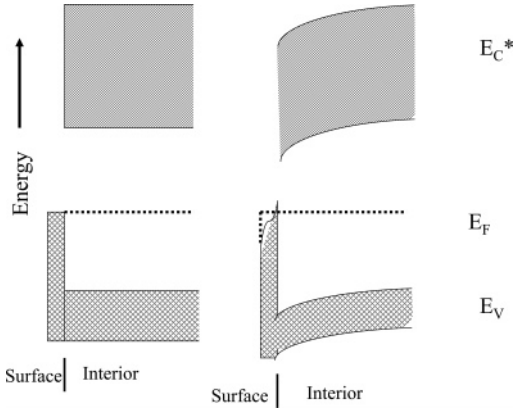


**Figure 3.** Energy distribution of surface and interior electrons for an ideal near-insulator crystal showing possible band bending.

valence and conduction bands labeled $A_2$, $A_{3A}$, $A_5$ and $C_2$, $C_3$, respectively, lying along the $X$, $M$, and $X'$ directions. The $A_3$ and $C_2$ surface states are located in the center of the bulk valance bands, and they remain essentially unchanged from compound to compound. On the other hand, the $C_3$ and $A_5$ surface states are present in the forbidden gap. These surface states are attributed to dangling bonds from both the empty cation ($C_3$) and the occupied anion ($A_5$). In general, these calculated results agree well with other theories and surface calculations.[11]

It is known that the electronic structures of semiconductors change with surface reconstruction and relaxation.[3] As a result, surface recombination rates as well as band bending are functions of the atomic rearrangement on the surface.[3,6] Also, the discontinuity of the conduction band throughout the distorted surface layers can result in free electrons becoming trapped, causing a space charge to build up.[12]

## 2.3. Surface States

Recombination of electron−hole pairs due to surface states is one pathway for nonradiative relaxation. Clean crystal surfaces may have a high density of localized levels in the band gap[5] due to the abrupt change at the surface of the 3D band structure associated with the bulk. States may also arise from impurity atoms or surface contamination that produces discrete quantum levels in the band gap near the surface.[5] As a result, measurements must take into account the effective values of both the bulk ($\tau_{bulk}$) and surface ($\tau_{surf}$) lifetimes: $1/\tau_{eff} = 1/\tau_{bulk} + 1/\tau_{surf}$. The surface lifetime is further discussed below in the surface recombination section.[5]

Not only may the surface band gap be different from the bulk, but band bending is affected by the presence of surface states. Depending upon the surface state density and energies, the Fermi level, $E_F$, is not always positioned between the valence and conduction bands. Depending on the nature of the material, the surface states may be only partially filled, as shown in Figure 3.[12] At equilibrium, $E_F^B$ in the bulk is equal to that of the solid surface, $E_F^S$. To accommodate this fact, the energy levels near the surface may be bent down or up depending on whether the semiconductor phosphor is n- or p-type.[12]

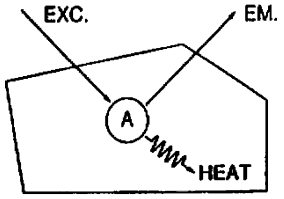


**Figure 4.** Direct excitation of the activator. Reprinted with permission from ref 2. Copyright 1994 Springer-Verlag.

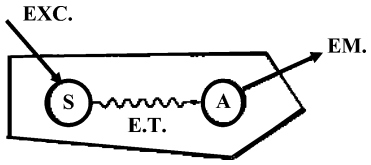


**Figure 5.** Diagram showing transfer of energy from the sensitizer, S, to the activator, A. Reprinted with permission from ref 2. Copyright 1994 Springer-Verlag.

Surface states or discontinuities can produce levels in the forbidden gap that extend hundreds of angstroms into the solid. Along with other distortions in the crystal, these states can be a source of closely spaced local levels that increase the rate of nonradiative transitions, reducing the efficiency of the phosphors.[12] The bonding position of surface atoms affects the energy positions of these surface quantum states, especially near the band gap. As shown in Figure 2 above, the calculated energy diagrams of Ferraz et al. show the energy dispersion of surface states in ZnS, ZnSe, and ZnTe.[11]

Several researchers have related bulk carrier accumulation in surface states to the development of strong surface electric fields. In essence, electron−hole pairs are created close to the surface region by photons or electrons. Hetrick et al. controlled the surface electric field using low-voltage biasing of Au−CdS Schottky barrier diodes. This allowed them to study the effects of surfaces on photoluminescence (PL) in n-type CdS. They found that surface electric fields hindered photoluminescence efficiency.[13] The three main factors which affected the field quenching of PL were surface charge, minority carrier surface recombination velocity, and intensity of the exciting light.[13] The surface states presumably were important through their influence upon the surface recombination velocity.

# *3. General Aspects of Luminescence*

## 3.1. Fundamental Luminescence Mechanisms

As discussed above and illustrated in Figure 1, luminescence results from release of energy as photons when electrons relax from high-energy (excited) to lower energy quantum states (often the ground state).[2,14,15] The luminescence may result from either a direct excitation or an energy transfer, as shown schematically in Figures 4 and 5.[2] Figure 4 shows a luminescent center, labeled activator (A), in a host lattice. By directly absorbing energy (i.e., from a photon or electron), an electron on A is raised to a higher energy state (band state, near-band edge state, or excited state; see Figure 1) and emits radiation as it relaxes back toward the ground state. As shown in Figure 5, the activator is not necessarily

always directly excited by the incoming energy. Excitation energy can be absorbed by the host lattice or a secondary ion, called the sensitizer, and then transferred to the activator to generate emission.

Luminescence processes are categorized on the basis of the method of excitation. PL occurs when the excitation sources are photons, typically short-wavelength or UV light. When energetic electrons excite the phosphor, the process is called CL. The application of an electric field across a phosphor which is sufficiently large to create ballistic charge transport is called electroluminescence (EL). Luminescence resulting from chemical reactions is labeled chemiluminescence. Ionoluminescence (IL) results from excitation by bombarding ions. When emission results from thermal excitation of an electron out of a deep trap after previous absorption of energy from a radiation source, the phenomenon is called thermoluminescence (TL). This list of mechanisms is not exhaustive; other types of luminescence include lyloluminescence (luminescence from solution), sonoluminescence (from sound), and triboluminescence (from friction, also known as mechanoluminescence (ML)), and the list continues. Each type of luminescence possesses its own unique excitation process and emission characteristics. In addition, the sensitivity of the luminescence mechanism to surfaces will vary considerably. In some cases, the sensitivity of the mechanism to surfaces is unknown. It is clear however that CL, EL, IL, ML, and PL processes are strongly affected by surface phenomena.

### 3.2. Concept of a Surface Dead Layer

While many aspects of the surfaces of phosphors affect luminescence brightness, efficiency, and lifetime, one aspect that has been discussed relative to all mechanisms is a luminescent "dead layer". For the case of CL and PL, the dead layer has usually been attributed to the presence of a surface space charge region.[15] In this layer, a high density of surface states exist that pin the Fermi level, causing a surface electric field. This field can physically separate electrons and holes (i.e., eliminate pairs), which will reduce the rate of radiative recombination by mechanisms 2−6 in Figure 1. Since radiative recombination rates are reduced, the electrons and holes are more likely to be trapped on nonluminescent centers and de-excited by nonradiative recombination.[15,16] Other researchers have attributed the dead layer effect to competition between drift and diffusion of electrons and holes.[17]

Historically, Wittry and Kyser used this concept of the dead layer to explain their observed dependence of CL intensity on electron beam voltage.[15,16] On the basis of the assumption that only nonradiative recombination occurs in this dead layer and since luminescence intensity is proportional to net excess carrier concentration, an expression for the CL efficiency was derived:

$$\eta_{CL} = \frac{\left[\int_d^{R_e} g(z_s)\,dz_s - \frac{S}{S+1}\int_d^{R_e} g(z_s)\,e^{-(z_s-d)/L}\,dz_s\right]}{\int_d^{R_e} g(z_s)\,dz_s} \quad (1)$$

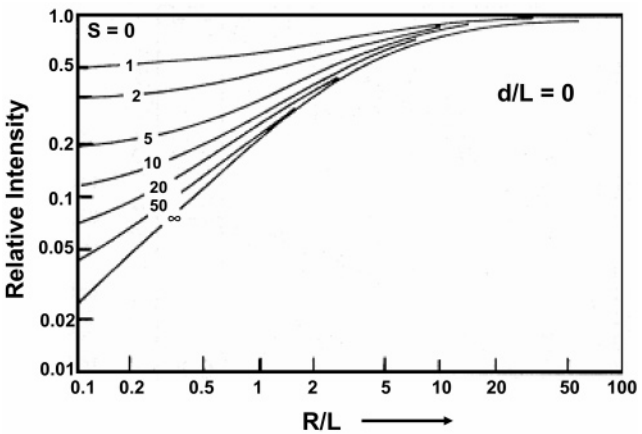


**Figure 6.** Calculated CL intensity plotted as a function of the reduced electron range and surface recombination velocity, assuming no dead layer is present. Reprinted with permission from ref 5. Copyright 1990 Plenum Press.

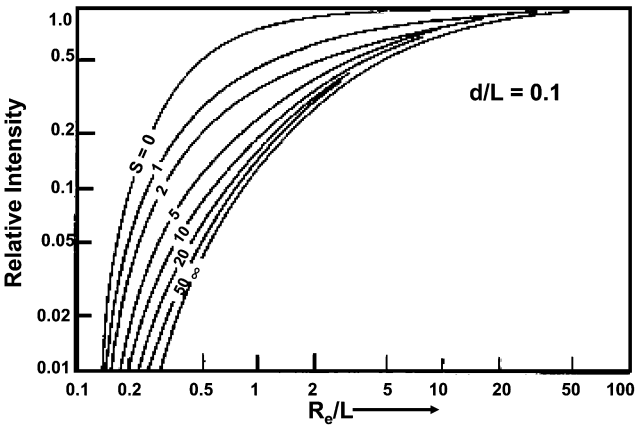


**Figure 7.** Calculated CL intensity as a function of reduced electron range, $R_e/L$, and surface recombination velocity, $S$, assuming a dead layer thickness of $d = 0.1L$. Reprinted with permission from ref 5. Copyright 1990 Plenum Press.

where $\eta$ = efficiency, $R_e$ = electron range, $S$ = reduced surface recombination velocity, $L$ = diffusion length, $d$ = dead layer thickness, and $g(z_s)$ = source depth distribution of excess carriers per unit depth.[15,16] The concept of a surface recombination velocity was introduced from semiconductor physics to complete the treatment. The concept of surface recombination is consistent with the presence of surface states, as discussed above. However, any phenomenon which leads to reduced radiative recombination rates near the surface will result in the same lower luminance. Wittry and Kyser used a finite surface recombination velocity in their model, even when a dead layer was not present (see below). Therefore, the concept of a dead layer will be introduced, followed by a more detailed discussion of the concept of surface recombination.

Wittry and Kyser calculated the CL intensity versus reduced electron range ($R_e/L$) for variable $S$ for Gaussian distributions of $g(z_s)$ as shown in Figures 6 and 7 for no dead layer ($d = 0$) and a dead layer defined by $d/L = 0.1$, respectively.[5,15,16] These results show that, if the primary electron beam range (energy) is too low, little or no CL intensity will be observed; i.e., the electron range (voltage) must exceed a threshold value to penetrate this dead layer.

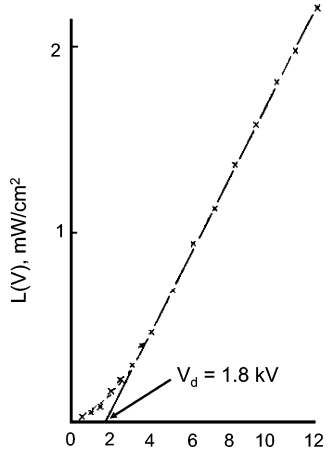


**Figure 8.** Cathodoluminescent brightness as a function of accelerating voltage Reprinted with permission from ref 18. Copyright 1960 Elsevier.

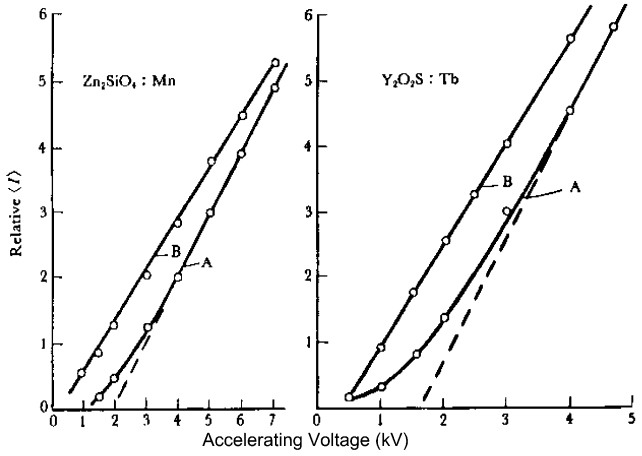


**Figure 9.** CL intensity vs accelerating voltage for (A) $Zn_2SiO_4$ and (B) $Y_2O_2S$:Tb screened phosphors: curve A, screened with binder; curve B, screened without binder. Reprinted with permission from ref 9. Copyright 1990 VCH Publishers.

After Gergely,[18] the threshold voltage from $L_{CL}$ versus accelerating voltage, $V$, in Figure 8 is defined to be the intercept of the $L(V)$ slope with the voltage axis.[18] Similary, dead voltage data from $Zn_2SiO_4$ and $Y_2O_2S$:Tb are shown in Figure 9.[9] Since $L_{CL}$ is seldom linearly dependent upon $I_b$ (electron beam current) at low voltages, Rao-Sahib and Wittry later modified both the experimental methods and theoretical curves. In actuality, $L_{CL} \propto I_b^m$, where $m$ lies between 1 and 2.[15,19] Assuming that the carrier generation rate does not vary with constant power density, at steady state Rao-Sahib and Wittry expressed the CL intensity as follows:

$$L_{CL} \cong \int_0^\infty [\Delta n(u)]^m \, du \tag{2}$$

and

$$u = \frac{\rho z}{R_e} \tag{3}$$

where $\Delta n$ = carrier density, $\rho$ = material density, $R_e$ = electron range, and $z$ = depth.[15,19]

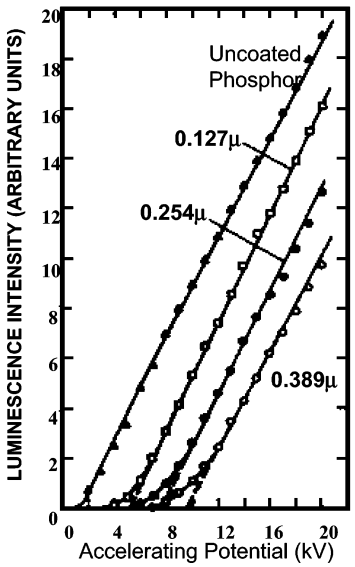


**Figure 10.** Cathodoluminescence vs voltage for ZnS-coated and uncoated ZnS:Cu. Reprinted with permission from ref 20. Copyright 1972 American Institute of Physics.

Rather than the presence of electric fields and surface recombination, some researchers attribute the dead layer to a high concentration of lattice defects. In this region a "dead voltage" exists corresponding to the condition of an electron beam range less than the depth of lattice defects and leads to the same concept of a threshold voltage.[7] Within the dead layer, nonradiative processes dominate over radiative processes, and the electron beam energy is dissipated near the surface. Both lattice defects and electrical charging may be present at the same time, since limited data suggest that, as electrical conductivity is increased, this dead voltage will decrease.[7,18]

Kingsley and Prener[20] reported a more direct demonstration of the dead layer phenomenon. They intentionally coated luminescent ZnS:Cu powder with an undoped, nonluminescent layer of ZnS. The coating varied in thickness from 0.1 to 0.5 $\mu$m as determined by weight.[20] There was a systematic loss of luminance and increase in the turn-on voltage as the coating thickness was increased. They showed that the reduced CL efficiency at low voltage resulted from power lost from the electron beam in the nonluminescent dead ZnS layer, if this dead layer was thicker than the carrier diffusion length. Plots of the CL luminescence intensity versus accelerating voltage from coated and noncoated samples are shown in Figure 10. A turn-on voltage of 1 kV was observed from unidentified causes for the noncoated phosphor. When a 0.12 $\mu$m coating of the nonluminescent ZnS was applied, the turn-on voltage increased to 3 kV.[20]

Similarly, Ohno and Hoshina examined the relationship between lower luminescence and surface oxidation of the surfaces of silica-coated ZnS:Ag, uncoated ZnS:Ag, and (ZnCd)S:Cu,Al. Growth of ZnO on the surface of the phosphors was reported to result from a reaction with a screening binder (ammonium dichromate). The powder samples were packed into metal trays and bombarded with a steady-state 10 kV electron beam at 0.5 $\mu$A/cm$^2$. As a result of this

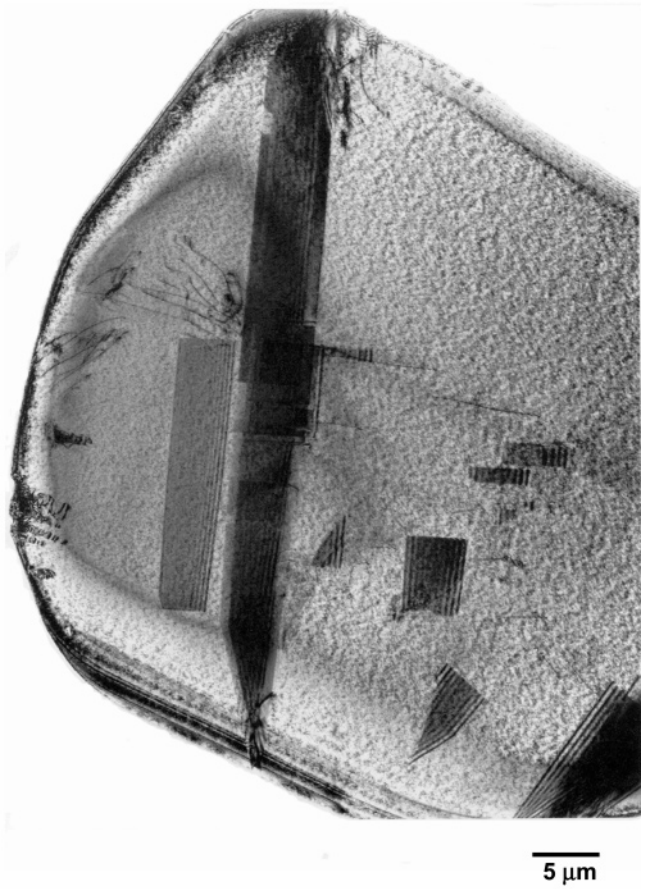


**Figure 11.** Bright-field TEM image of ZnS:Ag,Cl phosphor as-received. Reprinted with permission from ref 22. Copyright 2001 Slack.

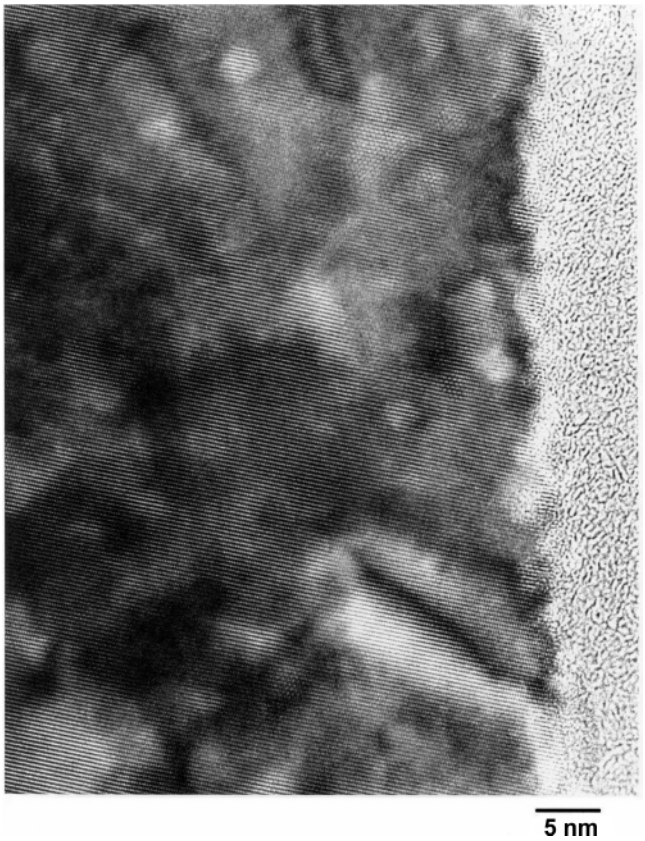


**Figure 12.** Lattice TEM image of as-received ZnS:Ag,Cl. Reprinted with permission from ref 22. Copyright 2001 Slack.

oxidation, they observed a reduction of the intrinsic luminescence efficiency.[21] These observations are similar to those reported below (section 6) of degradation of ZnS:Ag,Cl by surface chemical reactions stimulated by electron beam irradiation.

More recently, Kajiwara et al. have analyzed the surface dead layer of ZnS phosphor particles using TEM. After degradation by electron bombardment, the surface layer was highly defective as can be seen in Figure 11.[22] The first 10 nm of the particle reveals a high concentration of voids as well as a large root-mean-square roughness of $R_{rms} \approx 5$ nm (Figure 12).[22]

In summary, surface dead layers are widely observed and reported in the literature. The origins of these dead layers have been attributed to a variety of properties such as surface imperfections, surface states, surface oxidation, and surface charging. In the case of CL and PL, the dead layer effects are widely discussed in terms of surface recombination, which therefore will be discussed in more detail in the next section.

### 3.3. Decreased Luminance from Surface Recombination

It is clear that reduced luminescence is often observed when the excitation occurs near the surface of a phosphor, i.e., a surface dead layer is observed. For CL, this dead layer has been primarily attributed to surface recombination, which has been modeled to sophisticated levels. Due to dangling bonds at the surface, some researchers believe that it is covered by a layer of surface recombination (SR) centers.[9] The method for determining the depth of this SR layer is the same for determining the dead layer depth: measure the amount of carriers or luminescent intensity resulting from irradiation by an electron beam as a function of accelerating voltage. With this approach, it is assumed that, when the penetration depth of incoming electrons is less than the SR layer depth, there is little or no luminescence. Ozawa found a linear dependence of CL on accelerating voltages above 3 kV when analyzing phosphor screens of $Zn_2SiO_4$:Mn and $Y_2O_2S$:Tb. As can be seen in Figure 9, a dead voltage of 2 kV was determined. From this dead voltage, a dead layer thickness from surface recombination of 500 Å was calculated.[9] The thickness of the SR layer depended upon the method by which the phosphor was prepared.

As stated above, radiative and nonradiative lifetimes both affect the observed luminescent intensity. Since nonradiative processes are thought to be more likely at the surface, the effective lifetime is often written as a combination of surface and bulk lifetimes:[5]

$$\frac{1}{\tau_{eff}} = \frac{1}{\tau_{bulk}} + \frac{1}{\tau_{surf}} \quad (4)$$

If $\tau_{bulk}$ is long and $\tau_{surf}$ too short, surface recombination may dominate the lifetime and vary dependent upon the treatment experienced by the phosphor.

Surface recombination is also a function of temperature as described in the model of CL luminance by van Roosbroeck and Shockley:[5,23]

$$L_{CL} = \frac{8\pi n}{c^2}\left(\frac{A'}{A}\frac{1}{n_o} + \frac{1}{p_o}\right)\int_{\nu=0}^{\infty}\alpha(\upsilon)\upsilon^2 \times \exp\left(\frac{-h\nu}{kT}\right) Q(\nu)\, d\nu \int_{z=0}^{\infty}\Delta p(z)\exp[-\alpha(\nu)z]\, dz \quad (5)$$

where

$$\int_0^{\infty}\Delta p(z)\, dz = g\tau_p\int\psi(z)\, dz \quad (6)$$

$g$ = electron−hole pair generation rate, $\tau_p$ = total hole lifetime ($1/\tau_p = 1/\tau_{rr} + 1/\tau_{nr}$)

, $\tau_{rr}$ and $\tau_{nr}$ = the radiative and nonradiative relaxation time constants, respectively, $\psi(z)$ = diffusion equation solution for a particular generation function, surface recombination velocity, diffusion length ($L$), and $T$, $\Delta p(z)$ = excess minority carrier distribution, $A'/A$ = degeneracy factor, $\nu$ = radiation frequency, and $q(\nu)$ = detector quantum efficiency. To calculate $\Delta p(z)$, the continuity equation for diffusion of excess minority carriers must be used:[5]

$$D_p\frac{d^2\Delta p}{dz^2} - \frac{\Delta p}{\tau_p} + F(z) = 0 \quad (7)$$

Boundary conditions account for the diffusion of minority carriers to the surface:[5]

$$D_p\frac{d\Delta p}{dz} = s\Delta p(0) \quad (8)$$

where $s$ = surface recombination velocity which can be replaced by the reduced surface recombination velocity, $S = s\tau/L$. Taking this into account and substituting eqs 7 and 8 into eq 6, the CL intensity as a function of reduced range can be determined.[5] The reduced range is given by $W = R/\rho L$, and it varies depending on the value of $S$ for a Gaussian distribution.[5] Experimentally, the surface recombination velocity can be determined from the dependence of CL intensity on electron beam voltage.

Another approach to understanding the loss mechanism associated with surface recombination is by using the boundary condition for carrier diffusion to the surface:[5]

$$s\Delta n = D\left|\frac{\partial\Delta n}{\partial z}\right|_{z=0} \quad (9)$$

Van Roosbroeck derived the solution to this equation:[5,24]

$$\Delta n = \frac{G\tau}{2e(\pi d)^2 L}\int_0^{R_e}\left\{\exp\left[\frac{-|z - z_s|}{L}\right] - \frac{S-1}{S+1}\times \exp\left[-\frac{(z+z_s)}{L}\right]\right\} g(z_s)\, dz_s \quad (10)$$

where $\Delta n$ = stationary excess carrier density, $g(z_s)$ = source depth distribution of excess carriers per unit depth, $\Delta n(r)$ = excess minority carrier density, and $S$ = reduced surface recombination velocity. Figure 13 shows the predicted luminescence versus depth

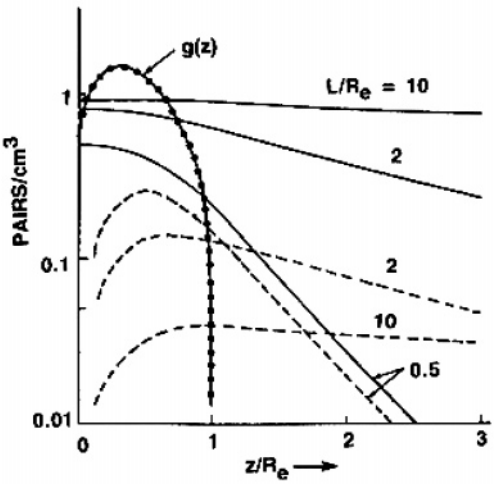


**Figure 13.** Generation rate, $g(z)$, versus reduced depth, $z/R_e$, for different carrier diffusion distances, $L/R_e$, and reduced surface recombination velocities, $S$: $S = 0$ (solid line) and $S = \infty$ (dashed line). Reprinted with permission from ref 5. Copyright 1990 Plenum Press.

from eq 10 when the surface recombination and carrier diffusion lengths are varied.[5,24] In this figure, the solid line ($S = 0$) represents the surface as a perfect reflector, whereas the dashed line ($S = \infty$) represents the surface as a perfect sink for charge carriers. Thus, surface recombination both reduces the electron−hole pair density near the surface and also leads to a lower total excitation level. Note that the effects of surface recombination are reduced for small values of $L$, i.e., by fast bulk recombination.

To determine the density of minority carriers lost to surface recombination, eq 10 must be differentiated with respect to $z_s$ and evaluated at $z = 0$:

$$\Delta n_s = \frac{S}{S+1}\int_0^{\infty}\exp\left(\frac{-z_s}{L}\right) g(z_s)\, dz_s \quad (11)$$

The loss of carriers due to surface recombination increases as $S/(S + 1)$. The loss decreases exponentially as $\exp(-z_s/L)$ if the generation range increases and/or the diffusion length decreases.[5,24]

If the time-dependent luminescent intensity, $L(t)$, decays exponentially, then a CL decay time can be determined that is influenced by surface recombination.[5] This CL decay can be expressed as follows:

$$L(t) = L(0)\exp\frac{-t}{\tau} \quad (12)$$

where the lifetimes, $\tau$, are effective values given by eq 4.[5,25] Hastenrath et al. calculated the minority carrier lifetime and the surface recombination velocity by measuring the CL decay time as a function of the electron beam energy (i.e., versus the electron penetration range).[26] From these measurements, they derived an expression for the surface recombination velocity:

$$S = L_p(\tau_{eff}^{-1} - \tau_0^{-1}) \quad (13)$$

where $L_p$ = hole diffusion length, $\tau_{eff}$ = effective lifetime, and $\tau_o$ = bulk lifetime.[5,26]

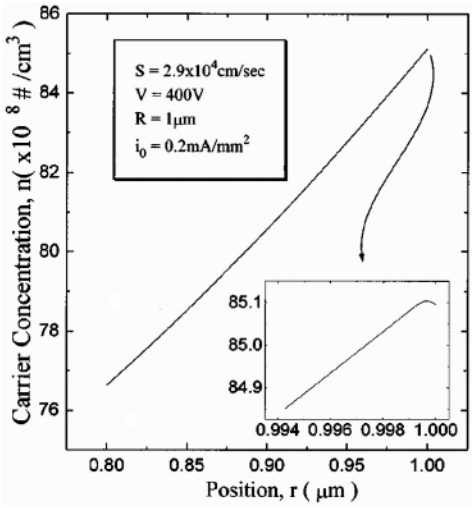


**Figure 14.** Carrier concentration versus depth with a surface recombination velocity of $2.9 \times 10^4$ cm/s. Reprinted with permission from ref 28. Copyright 1997 American Institute of Physics.

Other researchers have used a variety of techniques to quantify surface recombination phenomena. Jakubowicz et al. used a theoretical approach to analyze transient CL with a focused electron beam. They concluded that the initial decay depended on the surface recombination velocity, excitation range, and absorption coefficient, while the bulk lifetime controls the exponential decay at longer times.[27]

Yoo et al. used the diffusion equation characterizing the carrier concentration distribution to derive an expression for the brightness of a single spherical phosphor including surface recombination.[28] They were able to plot the relationship of the surface recombination rate and the carrier concentration versus position (Figure 14).[28] They concluded that reduced surface recombination rates are necessary to improve the phosphor efficiency.

Bukesov et al. developed a method to obtain recombination parameters for polycrystalline materials.[29] Their goal was to understand the effects of a coating on the phosphor surface. Similar to Yoo and Lee,[28] they used the diffusion equation to determine the distribution of minority carriers. Combining these data with a distribution function of the charge carriers, they were able to determine the surface recombination velocity by plotting CL intensity as a function of electron penetration depth, as shown in Figure 15.[29] Using this approach, they analyzed the effects of surface coatings on recombination velocities, and concluded that these parameters were sensitive to small amounts of coating material. Figure 16 demonstrates this sensitivity for $WO_3$ coating on the electric fields developed in the ZnO:Zn phosphor.[29]

Phang et al.[30] simulated the effects of surfaces on cathodoluminescence using a Monte Carlo method along with the Berz and Kuiken excess minority carrier distribution model. They incorporated the effects of surface recombination velocity, optical loss of photons at the surface, incident electron beam angle, and thickness of the surface dead layer.[30] Taking all of these factors into account, they were able to plot the change in CL efficiency as a function

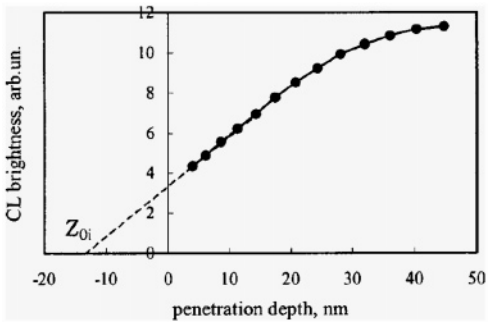


**Figure 15.** CL brightness as a function of electron beam penetration depth. Extrapolation to $Z_{0i}$ allows for determination of the surface recombination velocity. Reprinted with the permission of ref 29. Copyright 2002 American Institute of Physics.

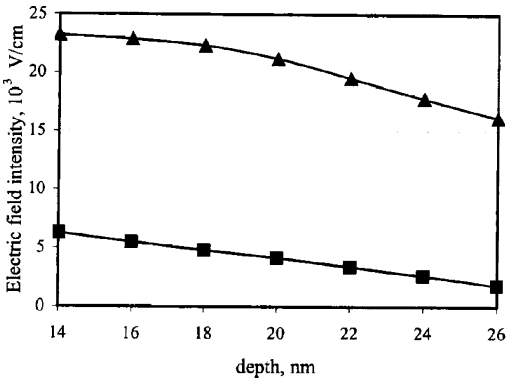


**Figure 16.** Electric field distribution in the ZnO:Zn surface layer with (■) and without (◆) a $WO_3$ coating. Reprinted with permission from ref 29. Copyright 2002 American Institute of Physics.

of surface recombination, absorption coefficient, and electron beam accelerating voltage. They found that surface recombination effects were directly related to the beam voltage and the absorption coefficient. An increase in the surface recombination velocity limits CL emission for high absorption coefficients since the only light capable of escaping is that generated near the surface (thus corresponding to a low accelerating voltage).[30]

Decreased phosphor efficiency due to surface recombination has been modeled in PL as well as in CL. In a study of efficiency of inorganic phosphors to soft X-rays, Benitez et al. found that nonradiative decay was dominated by surface recombination in addition to bulk trapping.[31] They applied a surface recombination model which allowed them to extract properties such as the diffusion length, reduced surface recombination velocity, and bulk quantum efficiency from the luminescence data.[31]

While in most cases surface recombination leads to a lower luminescence intensity due to nonradiative recombination, surfaces may lead to increased radiative transitions in some materials systems. Although the mechanism(s) of luminescence in porous silicon is controversial,[32] Hajnal et al. used an empirical tight binding (ETB) approximation to model the surface recombination during PL from porous silicon.[33] Their calculations suggested that local resonances in the conduction and valence bands were created by small "buds" on the silicon surface. Radia-

tive recombination enhanced by the surface resulted in photon emission from the carrier traps.

### 4. Surface Charging Effects on Luminescence

The existence of a surface electric field or surface charging was discussed above. The effect(s) of surface conductivity on luminescence has been difficult to separate from other surface effects such as recombination. Ozawa used the model of surface-bound electrons (SBEs) developed by Cole and Cohen to describe surface charging.[9,34] SBEs are defined as those electrons outside an insulator surface that are tightly bound to the positive charge that developed inside the surface volume of the crystal.[9] In CL, this positive charge is created by electron beam bombardment, which results in the ejection of secondary electrons (SEs) across the surface. When these SEs are ejected, holes representing a positive charge are left behind. A positive field is created, attracting true SEs which do not re-enter the crystal due to insufficient energy. Subsequently, they are bound a small distance outside the crystal surface, creating a negative space charge region.[9] This results in a decreased luminescence since the negative charge may act as a barrier to incoming low-energy electrons, presumably reducing the radiative recombination rate. Ozawa attributes the dead voltage (see section 2.2) to surface charging as well as to a surface recombination layer.

Feng et al. studied surface charging effects in the Ce:YAG phosphor.[35] They achieved surface charging by controlling secondary electron collection. The surface potential was altered by the accumulation of charge, affecting the incoming electron beam energy. Feng et al. concluded there were two components of surface charge: (1) uncollected secondary electrons held briefly on the surface, (2) charge trapped inside the active region of the bulk crystal. In the first case, the secondary electrons were termed "coating electrons" since they were loosely bound and easily attracted to another area of higher potential. In the second case, the "regionally active" charge was made up primarily of injected primary electrons, excited electrons, and holes. In the modeling of surface charge effects during electron beam bombardment, Feng et al. concluded that defect luminescence was affected more strongly than cerium luminescence.[35]

Seager et al. also explored the effect of an electric field upon CL intensities from several different phosphors: ZnS:Ag, $SrGa_2S_4$:Eu, ZnO:Zn, and $Y_2O_3$:Eu.[36] Their data show that a negative voltage at the surface led to increased CL intensities, while a positive voltage resulted in a reduced CL intensity. They initially attributed the CL increase to a reduced surface recombination rate, but later investigations led them to believe that surface charge reduction/accumulation was the cause of the CL increase/loss.[3,37]

### 5. Effects of Surface Chemical Reactions on Luminescence

Adsorption and desorption processes affect luminescence in many ways including modification of the work function, surface charge, and surface state characteristics and density.[15,38] Surface chemistry changes, such as adsorption, have led to luminescence quenching[38] through formation of SR centers. SR centers may quench CL by either (1) transfer of the radiative recombination to a new luminescence band or (2) increased nonradiative relaxation.[38]

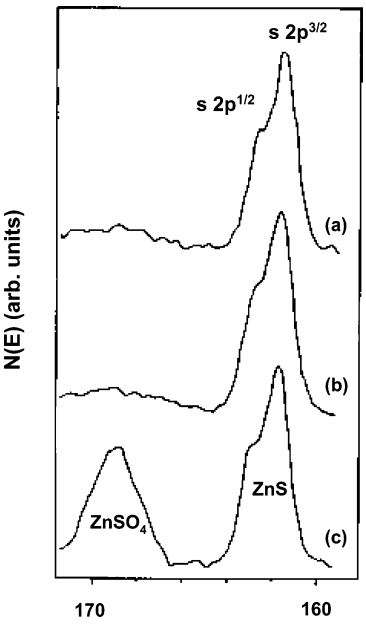


**Figure 17.** XPS data showing the conversion of ZnS to $ZnSO_4$. Reprinted with permission from ref 40. Copyright 1989 Electrochemical Society.

Many researchers have reported that surface chemical reactions can result in the formation of a surface dead layer, SR layer, surface morphological changes, or surface darkening. Surface darkening of $ZnS_{1-x}Cd_xS$:Ag,Al phosphors exposed to UV irradiation in a humid atmosphere was studied by Itoh et al.[39] A mercury arc lamp with a spot size focused down to about 2−3 cm was used to irradiate the phosphor surface. During irradiation, a notable decrease in photoluminescent intensity was observed. Even more prominent was a decrease in low-voltage cathodoluminescence intensities after the sample was exposed to the UV radiation. Using Auger electron spectroscopy (AES), X-ray photoelectron spectroscopy (XPS), and X-ray diffraction (XRD), the formation of $ZnSO_4$ and $CdSO_4$ and the precipitation of Zn and Cd colloidal metals were observed, suggesting that decomposition of the phosphor occurred near the surface.[39]

In studies of ZnS:Zn and $(Zn_{0.22}Cd_{0.78})$S:Ag,Cl powder phosphors for VFDs, Itoh et al. reported that they decomposed under electron beam bombardment while exposed to a background pressure of $5 \times 10^{-5}$ Torr of primarily water.[40] Using mass spectrometry, Itoh observed desorption of sulfur species from the phosphor surface as a result of exposure to low-energy electrons. Field emission scanning electron microscopy (FE-SEM), AES, and XPS data showed decomposition of the phosphor surface and formation of a $ZnSO_4$ surface dead layer (Figure 17). This dead layer formation was accelerated by the electron exposure in higher pressures of water and was reported to reduce the phosphor luminous efficiency.[40]

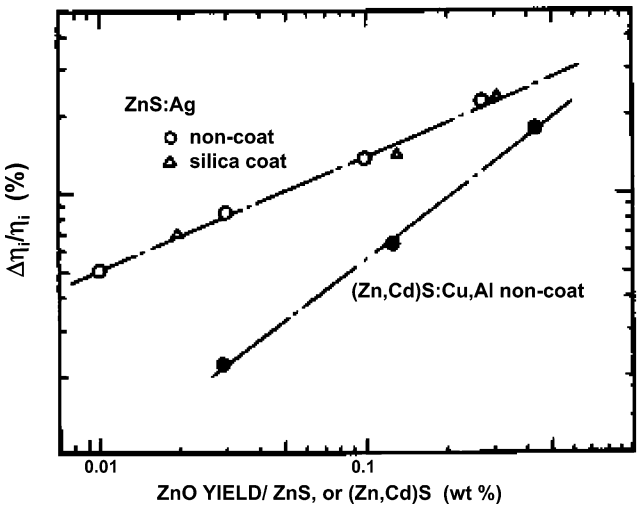


**Figure 18.** Loss of intrinsic luminescence as a function of ZnO yield. Reprinted with permission from ref 21. Copyright 1979 Electrochemical Society.

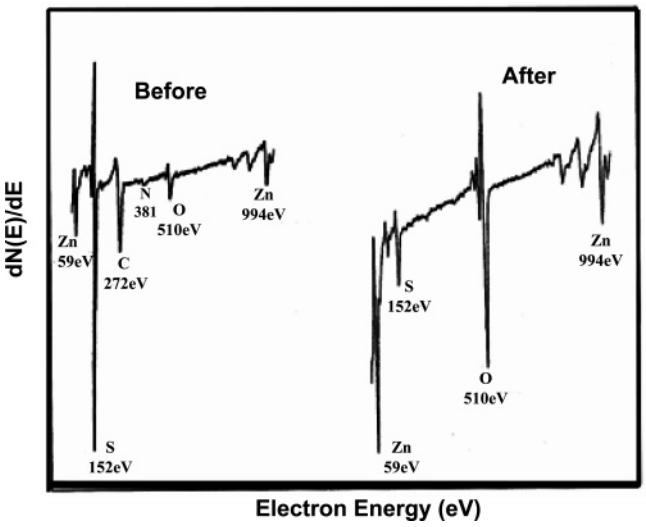


**Figure 19.** Auger spectra before and after degradation of ZnS. Reprinted with permission from ref 43. Copyright 1996 Slack.

Similar to this formation of a dead layer, Ohno and Hoshina examined the relationship between surface oxidation of silica-coated ZnS:Ag, uncoated ZnS:Ag, and (ZnCd)S:Cu,Al and loss of luminescence.[21] Transformation of the surface to ZnO resulted from a thermal reaction with the screening binder, ammonium dichromate (ADC). The reduction of the intrinsic luminescence efficiency as a result of this oxidation is shown in Figure 18.[21]

Formation of an electron-beam-induced dead layer on single-crystal ZnS(110) in the presence of water vapor was also reported by Okada et al.[41] AES data during 6 min of exposure to a 3 kV electron beam showed an increase of O and a decrease of S on the ZnS surface. This layer was only formed where the electron beam struck the ZnS film in the presence of water. On the basis of depth profiling data, the thickness of this layer was estimated to be about 600 Å.[41]

## 5.1. Electron-Stimulated Surface Chemical Reaction (ESSCR) Model

Electron-stimulated surface chemical reactions on phosphors were further investigated by Holloway et al. and Swart et al.[42,43] In analyzing the CL degradation behavior of ZnS:Cu,Al,Au and ZnS:Ag,Cl, AES and CL data were collected simultaneously during an extended period of electron beam exposure. This in situ characterization allowed a direct correlation between CL decay and changes in the surface chemistry. Degradation left the phosphor surface depleted of sulfur and rich in oxygen, as shown in the AES spectra of Figure 19, and is indicative of the formation of a ZnO surface dead layer. Due to these surface chemical changes, Swart and Holloway postulated that ESSCRs were occurring.[42,43] They suggested that the electron beam dissociated adsorbed $H_2O$ and $O_2$, converting them into reactive atomic species. These reactive atomic species combined with S at the surface, forming products with high vapor pressures such as $SO_x$, which would desorb from the surface and leave behind an increasingly thick, nonluminescent oxide (ZnO). Along with the formation of a surface dead layer, Sebastian et al.[44] postulated that subsurface point defects of isoelectronic oxygen on the sulfur sublattice were also created, which led to an increased probability of nonradiative recombination.[43]

A mathematical model of ESSCR was developed by Holloway et al. showing the dependence of degradation on the type of gas, gas pressure, current density, and electron beam energy.[45] Due to the low electron energy (~2 keV) and therefore short electron range, Holloway's model incorporated a surface science approach. A standard chemical reaction rate equation was used to express the rate of change of S concentration on the phosphor surface:

$$\frac{dC_s}{dt} = -kC_sC_{as}{}^n \tag{14}$$

where $C_s$ is the surface sulfur concentration, $k$ is a chemical rate constant, $C_{as}{}^n$ is the concentration of adsorbed atomic species that will react with ZnS, and $n$ is the order of the surface reaction, with first-order being assumed.[45] $C_{as}$ can be expressed as

$$C_{as} = Z\Phi_{ma}C_mJ\tau_{as} \tag{15}$$

where $Z$ is the number of reactive atomic species produced by disassociation of a molecule, $\Phi_{ma}$ is the cross section for dissociation and is a function of the electron beam energy $E_p$, $C_m$ is the concentration of surface molecular species, $J$ is the current density responsible for dissociation, and $\tau_{as}$ is the mean lifetime of the reactive atomic species.[45] This expression implies that the reaction for this process is rate limited by the adsorbed species production rate. The concentration of atomic species, $C_{as}$, is proportional to the concentration of molecular species, $C_m$, adsorbed onto the surface, which can be expressed as

$$C_m = \sigma\left(\tau_o \exp\left[\frac{Q}{kT}\right]\right)\left(\frac{P_m}{[2\pi mkT]^{1/2}}\right) \tag{16}$$

where $\sigma$ is the molecular sticking coefficient and is

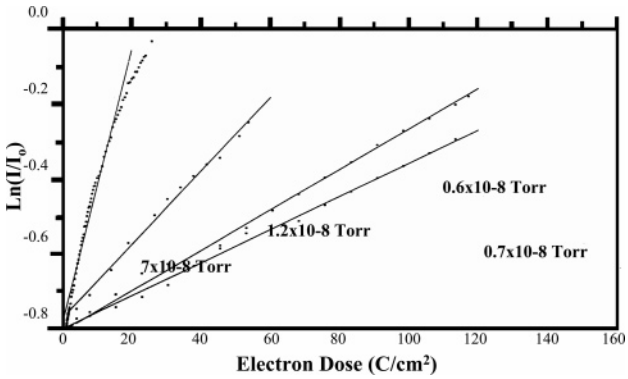


**Figure 20.** Semilogarithmic plot of CL vs electron dose for ZnS:Ag. Reprinted with permission from ref 42. Copyright 1996 Materials Research Society.

assumed to be independent of coverage. In this expression, the first bracketed term represents the mean stay time of a molecule on the surface, where $\tau_o$ is the mean time between escape attempts for adsorbed molecules, $Q$ is the surface desorption energy, $k$ is Boltzmann's constant, and $T$ is absolute temperature. The second bracketed term in eq 16 is the molecular flux onto the surface, where $P_m$ is the partial pressure of the molecular gas in the vacuum. After making the necessary substitutions of eqs 15 and 16 into eq 14, the reaction rate expression can be written as

$$\frac{dC_s}{dt} = -k\sigma C_s Z \Phi_{ma} J \tau_{as} \left(\tau_o \exp\left[\frac{Q}{kT}\right]\right)\left(\frac{P_m}{[2\pi mkT]^{1/2}}\right) \quad (17)$$

This expression can be written as follows:

$$\frac{dC_s}{C_s} = -K' J P_m \, dt \quad (18)$$

where

$$K' = k\sigma C_s Z \Phi_{ma} J \tau_{as} \left(\tau_o \exp\left[\frac{Q}{kT}\right]\right)([2\pi mkT]^{1/2}) \quad (19)$$

Finally, this equation may be integrated with respect to time, yielding

$$C_s = C_s{}^o \exp[-K' P_m J t] \quad (20)$$

where $C_s = C_s{}^o$ at $t = 0$, and the product of $J$ and $t$ is the Coulombic load.[45] With this model, the concentration of sulfur is predicted to decrease exponentially with Coulombic load. Assuming that the loss of sulfur is proportional to the loss of CL, the rate of CL degradation will increase with increasing gas pressure. These predictions are supported by the experimental data, as shown in Figure 20, which show that the CL intensity from ZnS:Cu decreases exponentially with increasing Coulombic dose and increasing pressure. Data in Figure 21 show that the Auger signal intensity from S also decreases exponentially with Coulombic dose after an "incubation" time attributed by Swart et al. to electron-stimulated removal first of carbon prior to sulfur reaction and removal.

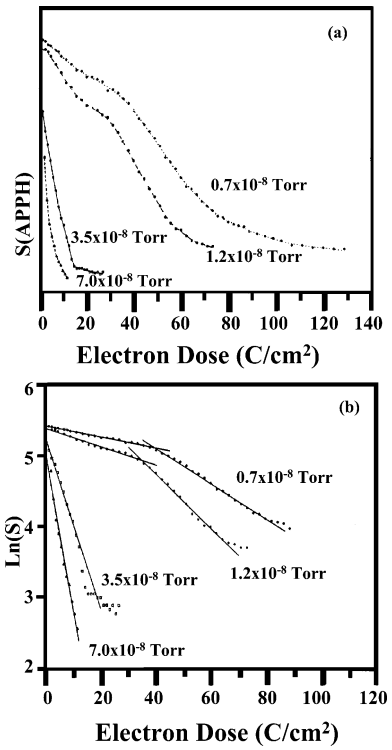


**Figure 21.** (a) Linear plot of sulfur AES peak height vs electron dose at 2 kV for ZnS:Ag and (b) semilogarithmic plot of (a). Reprinted with permission from ref 42. Copyright 1996 Materials Research Society.

## 5.2. Surface Dead Layer Formation and Growth

Similar surface changes were observed for a different materials system, $Y_2O_2S$:Eu.[42,45,46] Using AES and CL measurements under experimental conditions similar to those of Swart et al.,[43] S and C were depleted while O accumulated on the surface as a result of electron irradiation, implying that an oxide had replaced the oxysulfide layer, resulting in $Y_2O_3$:Eu. Unlike the ZnS-based systems where the oxide is nonluminescent, $Y_2O_3$:Eu formed under some conditions was luminescent as shown by emission at 612 nm ($Y_2O_3$) rather than 626 nm ($Y_2O_2S$). The conversion from $Y_2O_2S$:Eu prior to and from $Y_2O_3$:Eu after electron beam exposure is shown in Figure 22. This conversion explains the loss in CL intensity because $Y_2O_3$:Eu has a lower emission efficiency when compared with $Y_2O_2S$:Eu. To estimate the thickness of the oxide layer, the turn-on voltage was measured before and after degradation (see section 2.2). Using a modified Bethe equation for electron energy dissipation in a solid and Makhov's law for brightness as a function of power dissipation, Trottier et al. was able to calculate the dead layer thickness to be 860 Å.[42,45,46]

Cathodoluminescent degradation of SrS:Ce thin films versus Coulombic loading was studied by Abrams et al.[47] In a vacuum ambient dominated by oxygen, the process described by the ESSCR model was observed. After prolonged electron beam exposure, S was depleted from the surface and the O concentration was high. The thickness of the surface oxide layer was estimated using threshold voltage

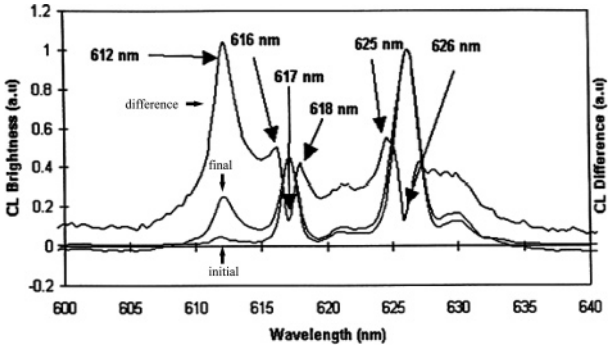


**Figure 22.** Cathodoluminescence spectra before and after degradation showing the conversion from $Y_2O_2S$:Eu to $Y_2O_3$:Eu. Reprinted with permission from ref 46. Copyright 2000 Society for Information Display.

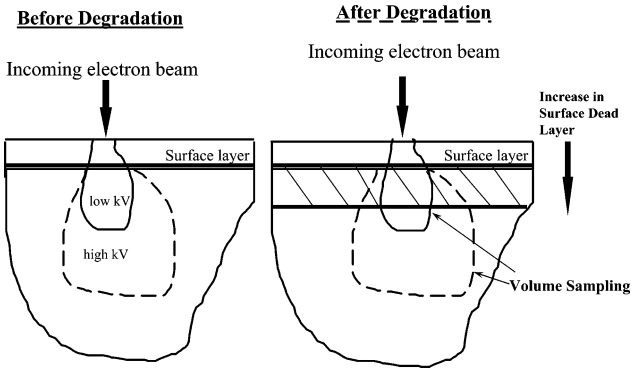


**Figure 23.** Schematic explanation of the threshold voltage measurement. Reprinted with permission from ref 14. Copyright 2001 University of Florida.

measurements and calculations as reported by Trottier et al.[45,46] As described in the schematic diagram of Figure 23[14] and in section 2.2, most phosphors possess an adventitious layer of physisorbed species because of exposure to air. This layer plus inherent surface defects leads to an initial dead layer of finite thickness. Electrons impinging on the sample surface result in an interaction volume, the size of which depends on the accelerating voltage and the properties of the material being excited. Before degradation, luminescence is generated in the volume beyond the initial dead layer. After degradation from prolonged electron beam exposure, the ESSCR promotes the growth of a thicker oxide dead layer, resulting in the need for a larger threshold voltage for excitation of CL.[14]

From the threshold voltage plot shown in Figure 24 and using the procedure described by Trottier et al., the dead layer thickness was found to increase by ~700 Å.[14,47] Abrams et al. measured the oxide thickness (presumably SrO) using Auger depth profiling both before and after degradation. The sputter rate for SrS:Ce, 100 Å/min, was determined by measuring the depth of a sputter crater in an undegraded area. The AES depth profiles taken before and after degradation, shown in Figures 25 and 26, show that the oxide layer thickness was increased by a thickness of ~700 Å, correlating well with the value calculated from the increased threshold voltage.[14,47]

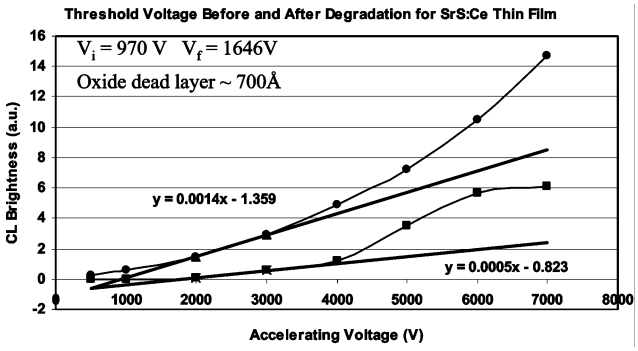


**Figure 24.** Threshold voltage plot of a SrS:Ce thin film showing CL brightness plotted as a function of accelerating voltage. Reprinted with permission from ref 47. Copyright 1998 Materials Research Society.

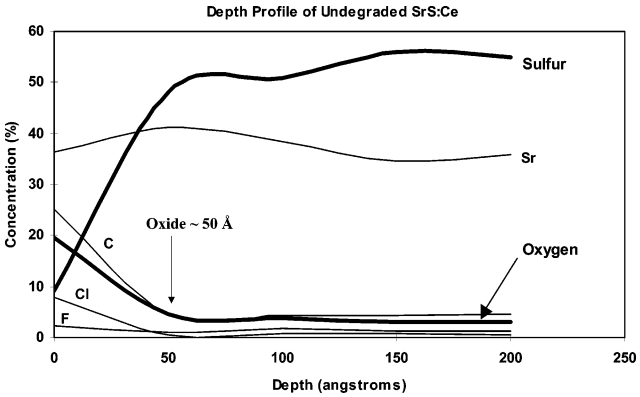


**Figure 25.** AES depth profile for SrS:Ce before degradation showing an initial oxide layer of 50 Å. Reprinted with permission from ref 47. Copyright 1998 Materials Research Society.

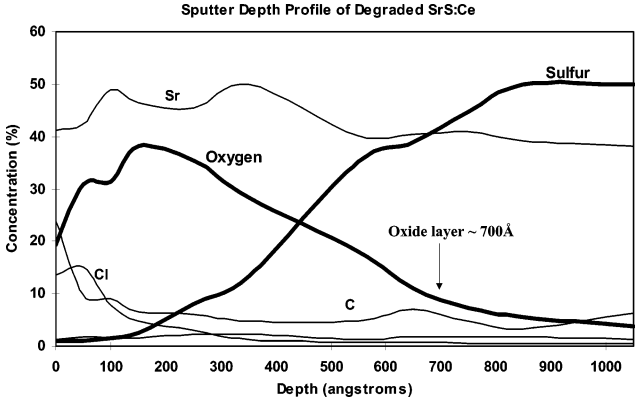


**Figure 26.** AES sputter depth profile of SrS:Ce after degradation showing an oxide dead layer of 700 Å. Reprinted with permission from ref 47. Copyright 1998 Materials Research Society.

## 5.3. Ambient Gas Effects

To gain more specific understanding of the role of specific gases in CL degradation and surface chemical reactions, the ZnS:Ag,Cl powder phosphor was exposed to electron beam bombardment in an ambient containing a high partial pressure of water monitored with a residual gas analyzer.[48] Residual gas analysis (RGA) spectra collected before, during, and after the experiment revealed a partial pressure of water of $\sim 1 \times 10^{-6}$ Torr. Degradation behavior similar to that reported by Swart et al. was observed, where S was

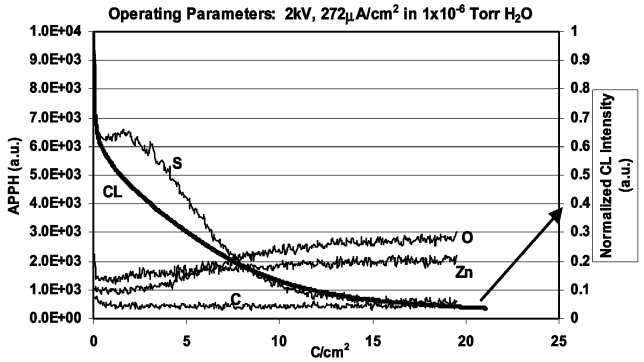


**Figure 27.** AES and CL trend data as a function of Coulombic loading for ZnS:Ag,Cl powder degraded in a high-water ambient. Reprinted with permission from ref 48. Copyright 2000 Elsevier.

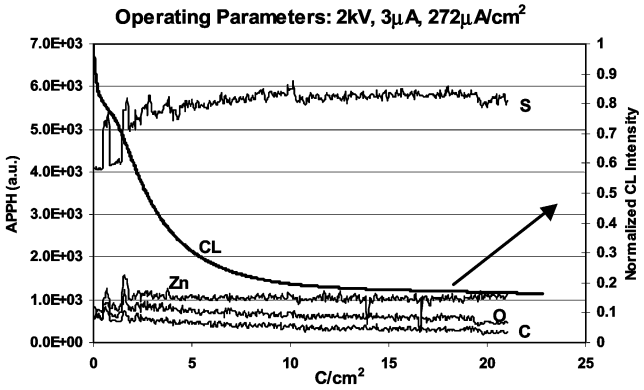


**Figure 28.** AES and CL trend data for ZnS:Ag,Cl powder degraded in a low-water, high-hydrogen ambient. Reprinted with permission from ref 48. Copyright 2000 Elsevier.

depleted and a surface oxide layer was formed. This is shown by the AES peak and CL intensity versus Coulombic dose data that are plotted in Figure 27.[14,48]

For comparison, the same phosphor was degraded in a vacuum ambient low in water (less than $1 \times 10^{-9}$ Torr). Following electron bombardment under the same conditions (2 kV, ~270 $\mu$A/cm$^2$) as in the case of high water pressure for a period of 24 h, the surface chemistry change was very different. For a low partial pressure of water, there was no decrease in the surface S signal and no increase in surface O, suggesting that no surface oxide layer was formed even though there was a significant loss of CL intensity (Figure 28).[14,48] While RGA data showed a low partial pressure of water, the partial pressure of hydrogen was greater than $2 \times 10^{-8}$ Torr. On the basis of these data, Abrams et al. concluded that electron-stimulated surface chemical reactions occurred in both cases with either $H_2$ or $H_2O$, whichever was greater. They developed a model describing an ESSCR involving $H_2$, as depicted in Figure 29. According to this model, physisorbed $H_2$ was dissociated by the electron beam into reactive atomic H. This atomic H reacted with surface S, desorbing from the surface, and leaving unbonded Zn which volatilizes because of its high vapor pressure. No oxide dead layer formed under these conditions, but the surface of the phosphor was driven nonstoichiometric and led to enhanced nonradiative recombination.

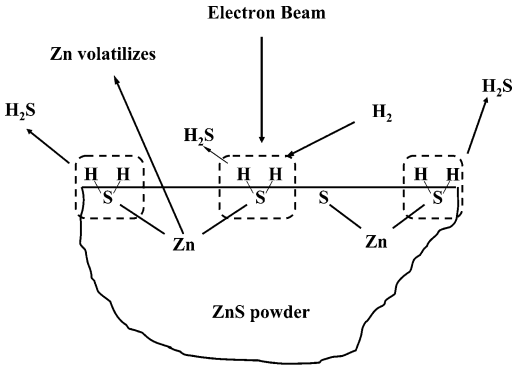


**Figure 29.** Schematic diagram of the ESSCR degradation model in a low-water, high-hydrogen ambient. Reprinted with permission from ref 48. Copyright 2000 Elsevier.

## 5.4. Surface Morphological Effects and Deterioration

Surface roughness and morphology are also factors that may either enhance or degrade luminescence emission. Rough surfaces can lead to local variations in optical absorption as well as reflection losses.[5] In some cases, surface roughness may enhance light scattering and result in an increased luminescent efficiency.

As reported above, Itoh et al. studied the degradation of ZnS:Zn and $(Zn_{0.22}Cd_{0.78})$S:Ag,Cl during CL.[40]

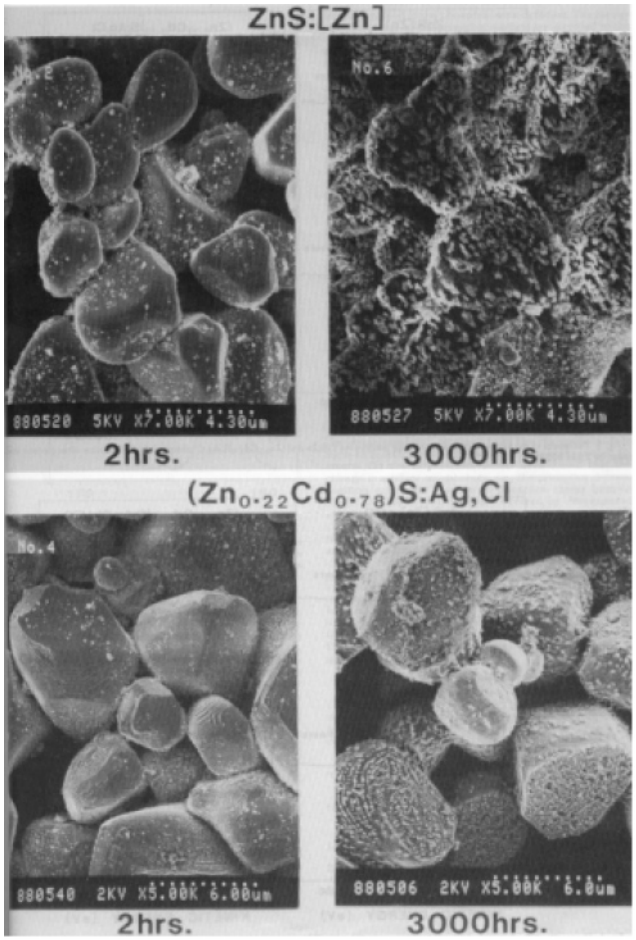


**Figure 30.** Surface morphological deterioration as a function of time exposure to the electron beam. Reprinted with permission from ref 40. Copyright 1989 Electrochemical Society.

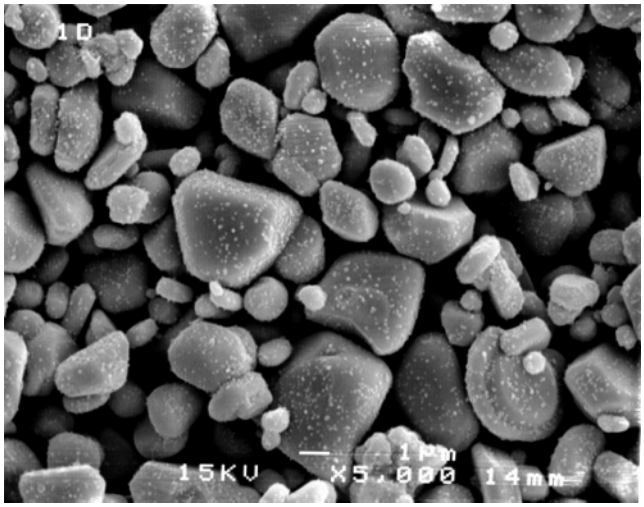


**Figure 31.** Scanning electron micrograph of a $SiO_2$-coated ZnS:Ag,Cl powder phosphor before degradation. Reprinted with permission from ref 48. Copyright 2000 Elsevier.

Along with observing the formation of a sulfate layer on the phosphor surface, Itoh observed changes in the morphology of the powder particles after prolonged electron beam exposure (Figure 30). This was attributed to decomposition and evaporation of the phosphor grains due to electron beam heating. The resulting roughened phosphor grains played a role in decreasing the luminous efficiency.[40]

In their study of the effects of ambient gas on CL degradation, Abrams et al. used SEM to analyze the phosphor morphologies before and after degradation.[14,48] Initially, ZnS:Ag,Cl powders coated with nanoparticulate $SiO_2$ were studied. Before electron beam exposure, the particles were fairly smooth with the exception of the nonuniform dispersion of $SiO_2$ nanoparticulates on the surface of the ZnS:Ag,Cl particles (Figure 31). After degradation at incrementally higher power densities (0.4, 0.5, 0.6, and 1.4 W/cm$^2$), the phosphor particles exhibited an increase in surface erosion, as can be seen in the SEM images in Figure 32.[14,48] Very apparent in these images is the concentration of erosion around the $SiO_2$ nanoparticulates. For comparison, the same set of experiments were performed on noncoated ZnS:Ag,Cl powder phosphors. In this case, no localized erosion developed after degradation, and the overall loss of CL intensity for the same Coulombic dose was less (by ~20%) than for the coated phosphors. Abrams et al. postulated that the surface $SiO_2$ nanoparticles acted as catalysts for degradation by ESSCRs, as shown in Figure 33.[14,48] Other nonuniform surface coatings were also tested, e.g., $TaSi_2$, Al, and $Al_2O_3$, and each resulted in similar characteristics; i.e., surface erosion was initiated around the nanoparticulates.[14] In each instance, electron-stimulated surface chemical reactions are initiated by dissociation of molecules into species that react with the surface, leaving it vulnerable to further reactions and sublimation.

The fact that surface erosion increases with increasing power density suggests that temperature could play an important role in ESSCR. This was studied by Abrams et al. on the basis of the ESSCR model. In this model, the effects of temperature were embedded in the expression for the molecular concentration of adsorbed surface species and the chemical reaction rate constant (eqs 16 and 14, respectively). However, the agreement between the model and experimental data suggests that the surface reactions are limited by the dissociation of molecular species, not by the rate of surface reaction by the atomic species. As a result, the predicted effects of temperature are contained within eq 16, and the main effect is an exponentially reduced molecular mean stay time and therefore a reduced concentration of atomic species with an increase in temperature. The ESSCR model predicts an increased flux of molecules onto the surface with increased temperature, but this is controlled by gas temperature

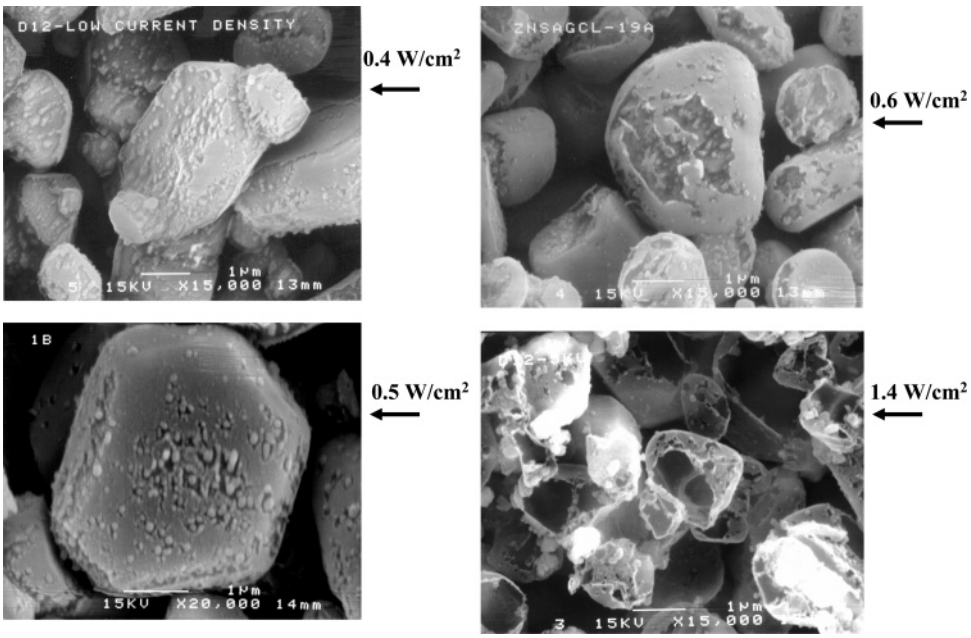


**Figure 32.** SEM images of the progression of morphological deterioration as the power density increases from 0.4 to 1.4 W/cm$^2$. Reprinted with permission from ref 14. Copyright 2001 University of Florida.

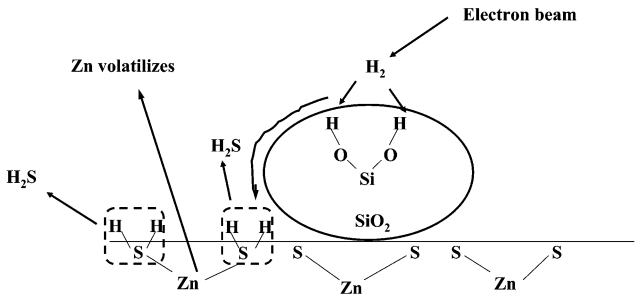


**Figure 33.** Schematic diagram of the ESSCR degradation model showing how $SiO_2$ nanoparticulates may act as a catalyst for degradation. Reprinted with permission from ref 48. Copyright 2000 Elsevier.

rather than substrate temperature, which would be little changed in most experiments. These predictions were supported by the data reported below.

To isolate the effects of temperature from acceleration of reactions due to surface nanoparticulates, Abrams et al. performed temperature experiments only on noncoated ZnS:Ag,Cl. Degradation of CL intensity was studied at temperatures up to 450 °C. It was established that the thermal quenching temperature for CL from ZnS:Ag,Cl was 150 °C.[14,49,50] In a typical experiment, the temperature of the phosphor was elevated, e.g., to 250 °C, and the phosphor was exposed to electron beam excitation at 2 kV and 300 $\mu$A/cm$^2$ for 24 h. The total CL intensity reduction after degradation and cooling to room temperature was less than the decrease in CL intensity during room-temperature degradation, consistent with the predictions from the ESSCR model.

Swart et al. and Darici et al. also observed reduced rates of surface chemical reactions on ZnS phosphors versus electron dose at elevated temperatures.[51,52] Darici et al. used AES to study the effects of electron bombardment on the surface of an undoped ZnS thin film in $1 \times 10^{-6}$ Torr of CO and $CO_2$ at temperatures ranging from room temperature to 200 °C.[51] When the ZnS film was exposed to an electron beam in a partial pressure of $CO_2$, C was deposited and S was removed at room temperature. When the sample temperature was increased from 150 to 200 °C, the deposition of C ceased due to a decrease in the mean stay time of the $CO_2$, consistent with the ESSCR model.[51]

While the ESSCR model predicts the effects of temperature upon the surface chemical reactions, it does not predict any changes in surface morphology. As shown for nanoparticulate-coated ZnS:Ag,Cl phosphors, the morphology changed dramatically upon degradation. The morphology of uncoated ZnS:Ag,Cl particles degraded at elevated temperatures was examined using SEM before and after degradation. As seen in Figure 34, dramatic erosion of the particle morphology took place during elevated temperature degradation. Similar to $SiO_2$-coated ZnS:Ag,Cl particles degraded at high power, the interior of the particle has "evaporated", leaving only a "shell" of the particle to be detected by SEM. This is consistent with the model postulated earlier for this degradation, i.e., ESSCR with hydrogen removing S (e.g., as $H_2S$), followed by thermal evaporation of unbonded

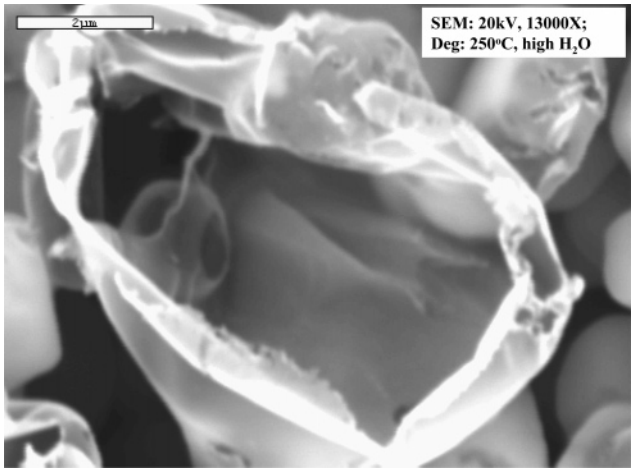


**Figure 34.** SEM image of noncoated ZnS:Ag,Cl powder after degradation at an elevated temperature (250 °C). Reprinted with permission from ref 14. Copyright 2001 University of Florida.

(or metallic bonded) Zn due to its high vapor pressure ($\sim 10^{-2}$ Torr at 300 °C).[14,49]

To further understand the role of temperature in ESSCR and CL degradation, the temperature rise due to electron beam heating was estimated. Due to the fact that the powders were loosely packed into the sample holders, there was very poor particle to particle contact to allow for efficient thermal conduction paths. Assuming that the heat generated by the energy input from the electron beam into a ZnS particle had only radiation as a dissipation path,[14,49] the Stefan equation for radiation was used:

$$q_r = \epsilon \sigma A_1 (T_1^4 - RT^4) \tag{21}$$

where $q_r$ = heat flow rate (W) (power), $\epsilon$ = emissivity, $A_1$ = surface area (m$^2$), $\sigma$ = Stefan−Boltzmann constant ($5.67 \times 10^{-8}$ W/(m$^2$ K$^4$)), $T_1$ = particle temperature (K), and $RT$ takes into account the room-temperature reverse radiation from the vacuum system walls. Under typical degradation conditions (2 or 5 kV, 3 or 5 $\mu$A electron beam), the electron beam impinges upon a phosphor particle that is ~5 $\mu$m in size. Thus, the input power per particle, $q_r$, is equal to

$$q_r = E_p J \left( \frac{\pi d_p^2}{4} \right) \tag{22}$$

where $J$ = electron beam current density (A/cm$^2$) and $d_p$ = ZnS particle size (cm). Equating $q_r$ in eqs 21 and 22 and solving for $T$, a temperature of ~150 °C was calculated for a 2 kV, 3 $\mu$A beam and ~240 °C for a 5 kV, 3 $\mu$A beam. These temperatures combined with external heating could cause a temperature rise of >300 °C. As stated above, the vapor pressure of Zn at this temperature is very high ($\sim 10^{-2}$ Torr), resulting in a very rapid removal of material, even for an uncoated phosphor.

The morphological deterioration observed by Abrams et al. and Itoh et al. creates a surface that is conducive to nonradiative recombination. In addition

to a nonstoichiometric composition, scattering of the luminescence will also contribute to degradation.

## 6. Surface Modification and Treatment

### 6.1. Processing of Powders

In the processing of powder phosphors for applications such as CRTs, FEDs, or lamps, the powders typically undergo some type of surface treatment. The particles may accumulate damage during processing such as grinding and baking. Generally, there are three reasons for treating the phosphor surface: (1) particle protection, (2) improving screening characteristics, and (3) improving contrast or pigmentation.[7] Particle protection addresses the issues of particle damage during processing or for surface reactions during CL, whereas improvement of screening and pigment characteristics relates more to deposition of the phosphor in the final device processing stages. In each case, the solution is often to apply a coating, either for protection or for pigmentation. Many authors have attempted to study the various effects of surface treatments of phosphors, including process parameters and coatings.

Itoh et al. studied the effects of grinding and baking processes on the luminescence of $Zn_{0.25}Cd_{0.75}S$:Ag,Cl mixed with $In_2O_3$.[53] Since this phosphor was being used in VFDs, the accelerating voltage of incoming electrons was very low, ~100 V. This led to a penetration depth for the electrons of ~10 Å, making the luminescence process very sensitive to surface effects and treatments. Itoh et al. reported that baking and grinding strongly influenced CL intensity by three main effects: (1) surface contamination, (2) strain, and (3) oxidation and decomposition of the phosphor surface.[53]

### 6.2. Coating of Phosphors

In an attempt to slow or eliminate luminescent and morphological degradation due to surface reactions, many researchers have applied coatings to the phosphor surface. However, as was demonstrated in section 5.4 on surface morphology, the coatings can be detrimental or beneficial to phosphor performance. This was also demonstrated by data from coating studies reported by Evans et al., who investigated the effects of ZnO coated on $SrGa_2S_4$:Eu,Pr and ZnCdS:Cu,Al.[54] They found no improvement, and in some cases degradation, of luminescence characteristics due to a noncontinuous surface coating.

Other researchers had more success with coatings on phosphor powders. Lee et al. coated ZnS:Ag with MgO and coated $Y_2SiO_5$:Ce with $In_2O_3$, $Al_2O_3$, and $SiO_2$.[55] They found that the CL efficiency was improved for the MgO-coated ZnS:Ag and the $Al_2O_3$- and $SiO_2$-coated $Y_2SiO_5$:Ce. However, the efficiency decreased for the $In_2O_3$ coating of $Y_2SiO_5$:Ce.[55]

Kominami et al. mixed ZnS:Ag,Cl phosphor powder with $In_2O_3$ and also applied a 10 nm thick layer of $In_2O_3$ to the ZnS:Ag,Cl phosphor powder using sol−gel methods and reported an increase in brightness.[56,57] They attributed this to the conductive properties of the coating, which decreased surface charging. The coating also resulted in slower aging rates.[56,57]

The effects of coating ZnS:Ag,Cl with blue $Cu_xS$ were investigated by Yang et al.[58] They found that the CL intensity of the coated phosphor improved depending upon heat treatment conditions. The CL intensity was reduced due to oxidation of the phosphor if it was baked at high temperatures.[58]

Park et al. studied $SiO_2$-coated ZnS in an attempt to reduce surface-related luminescence losses.[59] They used sol−gel processing to completely encapsulate the phosphor particles. The 5 nm thick surface coating was uniform and continuous, containing no individual $SiO_2$ particulates. For CL at <500 V, their best results showed a 60% increase in efficiency. This was attributed to a decrease in surface recombination.

Igarashi et al. deposited ZnO nanoparticles using a colloidal chemistry method onto ZnS:Ag,Cl in an attempt to decrease CL degradation.[60] For a very low Coulombic loading, they reported a decrease in the initial rate of degradation. This initial degradation is thought to be due to either charging or thermal quenching. It is known that the thermal and electrical conductivities of ZnO are better than those of ZnS. Thus, the decrease in degradation was attributed to a suppression of electron beam heating effects as well as reduced surface charging.[60]

Coating has also been used to enhance EL. Nakamura et al. coated ZnS phosphor particles with $BaTiO_3$ using sol−gel processing.[61] The EL cells that used this coating were reported to have an order of magnitude lower resistance and higher EL brightness versus noncoated phosphor.[61]

### 6.3. Thin Film Deposition and Surface Treatment

The discussion above has emphasized the effects of the surface in powder phosphors. However, the effects of processing and surface treatments on thin films have also been studied. For CL applications, thin films have exhibited a dramatically lower efficiency when compared to powders. This low efficiency is mainly due to light piping or total internal reflection effects. Attempts to improve the thin film phosphor efficiency by changing the surface morphology have met with some success. Jones et el. have shown that, by increasing the surface roughness, the CL intensity and efficiency of $Y_2O_3$:Eu thin films can be increased.[62,63] The surface was roughened both by growth on a mechanically roughened substrate and by increasing the $O_2$ pressures during pulsed laser deposition of the $Y_2O_3$:Eu phosphor thin films.[62,63] The PL intensity from the films was measured after depositions at varying $O_2$ partial pressures. The greatest increase in PL intensity was observed for an oxygen pressure range of 200−600 mTorr.[62,63] The rms roughness was 70 nm for an $O_2$ pressure of 600 mTorr, and was correlated with an order of magnitude increase in brightness due to forward scattering of luminescence. Similar effects were observed for CL intensity versus roughness.

As in the case of low-voltage band edge recombination EL, a smooth, clean surface is preferred to enhance luminescence. Along these lines, the surface

preparation of ZnSe crystals used for optoelectronic devices was studied by Garcia et al.[64] They reported that the PL was affected by the surface states and that surface treatment prior to PL measurements could modify the influence of these surface states. Using mechanochemical polishing, the surface quality was improved, which resulted in higher PL brightness.[64]

The effects of surface treatment of ITO on organic EL devices was investigated by Ishii et al.[65] and Liu et al.[66] Ishii et al. reported improved performance and lower operating voltages for low-voltage organic EL devices when the ITO surface was plasma treated. They suggested that this was due to an increase in the work function of ITO from 4.5 to ~6 eV. This change in the work function was correlated with removal of surface carbon contamination by plasma treatment.[65] Liu et al. studied four different surface treatment methods and used the Taguchi method to optimize[66] the effects of mechanical, chemical, UV-ozone, and $O_2$ plasma surface treatments.[66] They found the most improvement (>50%) with a combination of mechanical polishing and $O_2$ plasma treatments.[66]

On the basis of these studies, surface treatment is a viable method for enhancement of luminescence from CL, PL, and EL. The type of treatments will depend on whether the phosphor is a thin film or powder. For powders, protection from contamination, surface erosion, surface chemical reactions, charging, and heating are factors to consider when choosing a surface treatment method. For thin films, the surface treatment process is dependent upon the application. In some cases, surface roughening enhances luminescence (i.e., CL). In other cases, a clean, smooth surface with no defects increases luminescence brightness (i.e., EL).

## 7. Conclusions

The importance of surfaces to luminescence has been discussed. The understanding of surface properties has improved over the past several years in phosphors, but particularly in the area of semiconductors. It is clear that the composition, crystal structure, and electronic structure of the surface may and often will be different from the bulk properties. Segregation of activators to surfaces of phosphors has been demonstrated, and the effects of surface states have been demonstrated by empirical data and their interpretation. The consequences of the surface states on phosphors have been largely modeled in terms of a surface dead layer or surface recombination. It is clear that it would be beneficial to document the critical parameters important to these phenomena, and that they should be modeled on the basis of first principles and well-established materials principles. An example of predictive model development is that of ESSCRs, which allow predictions for critical parameters such as gas pressure, temperature, primary beam energy, etc. While some aspects of the ESSCR model have been tested, it would be wise for it to be tested more quantitatively by several different research groups. Models similar to the ESSCR model have been developed for surface recombination effects on luminescence, based upon recombination effects in semiconductors. In contrast to semiconductors where predictions based on the model have been tested on electrical properties and performance, there is a need for more detailed testing in terms of luminescent properties.

## 8. Acknowledgments

Sandia is a multiprogram laboratory operated by Sandia Corp., a Lockheed Martin Co., for the U.S. Department of Energy under Contract DE-AC04-94AL85000.

## 9. References

(1) Harvey, E. N. *A History of Luminescence From the Earliest Times Until 1900*; J. H. Furst Co.: Baltimore, MD, 1957.
(2) Blasse, G.; Grabmaier, B. C. *Luminescent Materials*; Springer-Verlag: Berlin, 1994.
(3) Holloway, P. H.; Thomes, W. J.; Abrams, B.; Jones, S.; Williams, L. *7th International Display Workshops—IDW'00*, Kobe, Japan, 29 Nov to 1 Dec 2000; Inst. Image Inf. & Telev. Eng. & Soc. Inf. Display (SID): Tokyo, Japan, and San Jose, CA, 2000.
(4) Brundle, C. R.; Evans, C. A.; Wilson, S. *Encyclopedia of Materials Characterization*; Manning Publications Inc.: Greenwich, CT, 1992.
(5) Yacobi, B. G.; Holt, D. B. *Cathodoluminescence Microscopy of Inorganic Solids*, 1st ed.; Plenum Press: New York, 1990.
(6) Hudson, J. B. *Surface Science An Introduction*, 1st ed.; Butterworth-Heinemann: Stoneham, MA, 1992.
(7) *Phosphor Handbook*; Shionoya, S. Y. W. M., Ed.; CRC Press LLC: Boca Raton, FL, 1999.
(8) Jones, S. L.; Kumar, D.; Cho, K. G.; Singh, R.; Holloway, P. H. *Displays* **1999**, *19*, 151.
(9) Ozawa, L. *Cathodoluminescence Theory and Applications*; Kodansha Ltd., VCH Verlagsgesellschaft mbH, VCH Publishers: Tokyo, Japan; Weinheim, Germany; New York,, 1990.
(10) Gadzuk, J. W. *Surf. Sci.* **1975**, *53*, 132.
(11) Ferraz, A. C. W. K.; Alves, J. L. A. *Surf. Sci.* **1994**, *307−309*, 959.
(12) Leverenz, H. W.; Seitz, F. *J. Appl. Phys.* **1939**, *10*, 479.
(13) Hetrick, R. E.; Yeung, K. F. *J. Appl. Phys.* **1971**, *42*, 2882.
(14) Abrams, B. L. Ph.D. Dissertation, University of Florida, 2001.
(15) *Luminescence of Solids*; Vij, D. R., Ed.; Plenum Press: New York, 1998.
(16) Wittry, D. B.; Kyser, D. F. *J. Appl. Phys.* **1967**, *38*, 375.
(17) Goulding, F. S. *Nucl. Instrum. Methods* **1977**, *142*, 213.
(18) Gergely, G. Y. *J. Phys. Chem. Solids* **1960**, *17*, 112.
(19) Rao-Sahib, T. S.; Wittry, D. B. *J. Appl. Phys.* **1969**, *45*, 5060.
(20) Kingsley, J. D.; Prener, J. S. *J. Appl. Phys.* **1972**, *43*, 3073.
(21) Ohno, K. H., T. *J. Electrochem. Soc.* **1979**, *126*, 1975.
(22) Kajiwara, K. *J. Vac. Sci. Technol., A* **2001**, *19*, 1083.
(23) Van Roosbroeck, W.; Schockley, W. *Phys. Rev.* **1954**, *94*, 1558.
(24) Van Roosbroeck, W. *J. Appl. Phys.* **1955**, *26*, 380.
(25) Schockley, W. *Electrons and Holes in Semiconductors*; Van Nostrand: Princeton, NJ, 1950.
(26) Hastenrath, M.; Kubaleck, E. *Scanning Electron Microsc.* **1982**, 157.
(27) Jakubowicz, A. *J. Appl. Phys.* **1985**, *58*, 4354.
(28) Yoo, J. S.; Lee, J. D. *J. Appl. Phys.* **1997**, *81*, 2810.
(29) Bukesov, S. A.; Jeon, D. Y. *Appl. Phys. Lett.* **2002**, *81*, 2184.
(30) Phang, J. C. H.; Pey, K. L.; Chan, D. S. H. *IEEE Trans. Electron Devices* **1992**, *39*, 782.
(31) Benitez, E. L.; Husk, D. E.; Schnatterly, S. E.; Tarrlo, C. *J. Appl. Phys.* **1991**, *70*, 3256.
(32) Ludwig, M. H. *Crit. Rev. Solid State Mater. Sci.* **1996**, *21*, 265.
(33) Hajnal, Z.; Deak, P. *J. Non-Cryst. Solids* **1998**, *227−230*, 1053.
(34) Cole, M. W.; Cohen, M. H. *Phys. Rev. Lett.* **1969**, *23*, 1234.
(35) Feng, X. D.; Warde, C. *J. Appl. Phys.* **1993**, *73*, 3926.
(36) Seager, C. H.; Warren, W. L.; Tallant, D. R. *J. Appl. Phys.* **1997**, *81*, 7994.
(37) Seager, C. H. *Appl. Phys. Lett.* **1998**, *73*, 85.
(38) Wolkenstein, T. *Electronic Processes on Semiconductor Surface During Chemisorption*; Consultants Bureau: New York, 1991.
(39) Itoh, S.; Tonegawa, T.; Morimoto, K. *J. Electrochem. Soc.* **1987**, *134*, 2628.
(40) Itoh, S.; Kimizuka, T.; Tonegawa, T. *J. Electrochem. Soc.* **1989**, *136*, 1819.

(41) Okada, A. O.; Takao. *J. Appl. Phys.* **1979**, *50*, 6934.
(42) Holloway, P. H.; Sebastian, J.; Trottier, T.; Jones, S.; Swart, H.; Peterson, R. O. In *Symposium on Flat Panel Display Materials II*, MRS Proceedings, San Francisco, CA, April 8−12, 1996; Hatalis, M., Kanicki, J., Summers, C., Funada, F., Eds.; Materials Research Society: Warrendale, PA, 1997; p 425.
(43) Swart, H. C.; Sebastian, J. S.; Trottier, T. A.; Jones, S. L.; Holloway, P. H. *J. Vac. Sci. Technol., A* **1996**, *14*, 1697.
(44) Holloway, P. H.; Trottier, T. A.; Abrams, B.; Kondoleon, C.; Jones, S. L.; Sebastian, J. S.; Thomes, W. J. *J. Vac. Sci. Technol.* **1999**, *17*, 758.
(45) Holloway, P. H.; Trottier, T. A.; Sebastian, J.; Jones, S.; Zhang, X.-M.; Bang, J.-S.; Abrams, B.; Thomes, W. J.; Kim, T.-J. *J. Appl. Phys.* **2000**, *88*, 1.
(46) Trottier, T. A.; Krisnamoorthy, V.; Abrams, B.; Fitzgerald, J.; Singh, R.; Zhang, X.-M.; Petersen, R.; Holloway, P. *J. Soc. Inf. Display* **2000**, Suppl. 1, 217.
(47) Abrams, B. L.; Trottier, T. A.; Swart, H. C.; Lambers, E.; Holloway, P. H. *Mater. Res. Soc. Symp. Proc.* **1998**, *508*, 261.
(48) Abrams, B. L.; Roos, W.; Holloway, P. H.; Swart, H. C. *Surf. Sci.* **2000**, *451*, 174.
(49) Abrams, B. L.; Williams, L.; Bang, J.-S.; Holloway, P. H. *J. Electrochem. Soc.*, to be published.
(50) Abrams, B. L.; Williams, L.; Bang, J.-S.; Holloway, P. H. *J. Appl. Phys.*, submitted for publication.
(51) Darici, Y.; Holloway, P. H.; Sebastian, J. S.; Trottier, T.; Jones, S.; Rodriguez, J. *J. Vac. Sci. Technol., A* **1999**, *17*, 692.
(52) Swart, H. C.; Hillie, K. T.; Greeff, A. P. *Surf. Interface Anal.* **2001**, *32*, 110.
(53) Itoh, S.; Tonegawa, T.; Pykosz, T. L.; Morimoto, K.; Kukimoto, H. *J. Electrochem. Soc.* **1987**, *134*, 3178.
(54) Evans, D. R.; Warren, G. T.; Raukas, M.; Happek, U.; Dennis, W. M.; Sun, S. S.; Basun, S.; Kane, J.; Yocom, P. N.; Naman, A.; Holloway, P. First International Conference on the Science and Technology of Display Phosphors, San Diego, CA, November 14−16, 1995; *J. Soc. Inf. Disp.* **1998**, *6* (1), 9.
(55) Lee, R. Y. K., S. W.; Kang, S. S. *J. Lumin.* **2001**, *93*, 93.
(56) Kominami, H.; Nakamura, T.; Sowa, K.; Nakanishi, Y.; Hatanaka, Y.; Shimaoka, G. *Appl. Surf. Sci.* **1997**, *113*/*114*, 519.
(57) Kominami, H. N., Takato; Hatanaka, Yoshinori. *Jpn. J. Appl. Phys.* **1996**, *35*, L1600.
(58) Yang, S.-H.; Yokoyama, M. *J. Vac. Sci. Technol., A* **1998**, *16*, 3443.
(59) Park, W.; Wagner, B. K.; Russell, G.; Yasuda, K.; Summers, C. J. *J. Mater. Res.* **2000**, *15*, 2288.
(60) Igarashi, T.; Kusunoki, T.; Ohno, K.; Isobe, T.; Senna, M. *Mater. Res. Bull.* **2001**, *36*, 1317.
(61) Nakamura, T.; Kamiya, M.; Watanabe, H.; Nakanishi, Y. *J. Electrochem. Soc.* **1995**, *142*, 949.
(62) Holloway, P. H.; Jones, S. L. *J. Surf. Anal.* **1998**, *3*, 226.
(63) Jones, S. L. Ph.D. Dissertation, University of Florida, 1997.
(64) Garcia, J. A.; Munoz, V.; Martinez-Tomas, C.; Garitanonandia, J. J. S. *J. Mater. Res.* **2001**, *16*, 1245.
(65) Ishii, M.; Mori, T.; Fujikawa, H.; Tokito, S.; Taga, Y. *J. Lumin.* **2000**, *87*−*89*, 1165.
(66) Liu, J.-M.; Lu, P.-Y.; Weng, W.-K. *Mater. Sci. Eng.* **2001**, *B85*, 209.

CR020351R